

N73-10002

NASA TECHNICAL NOTE



NASA TN D-7069

NASA TN D-7069

COPY

AERODYNAMIC CHARACTERISTICS OF  
A SWEEP-WING CRUISE MISSILE AT  
MACH NUMBERS FROM 0.50 TO 2.86

*by M. Leroy Spearman and Ida K. Collins*

*Langley Research Center*

*Hampton, Va. 23365*

1. Report No. NASA TN D-7069	2. Government Accession No.	3. Recipient's Catalog No.	
4. Title and Subtitle AERODYNAMIC CHARACTERISTICS OF A SWEEP-WING CRUISE MISSILE AT MACH NUMBERS FROM 0.50 TO 2.86		5. Report Date November 1972	6. Performing Organization Code
		8. Performing Organization Report No. L-8508	
7. Author(s) M. Leroy Spearman and Ida K. Collins		10. Work Unit No. 760-67-81-03	11. Contract or Grant No.
9. Performing Organization Name and Address NASA Langley Research Center Hampton, Va. 23365		13. Type of Report and Period Covered Technical Note	
		14. Sponsoring Agency Code	
12. Sponsoring Agency Name and Address National Aeronautics and Space Administration Washington, D.C. 20546		15. Supplementary Notes	
16. Abstract  An investigation has been made in the Mach number range from 0.50 to 2.86 to determine the longitudinal and lateral aerodynamic characteristics of a cruise missile having a 58° swept wing and conventional aft tails. Such a vehicle might be applicable to missions such as surface- or air-launched tactical or strategic missiles, unmanned reconnaissance, or countermeasure decoys.			
17. Key Words (Suggested by Author(s)) Cruise missile Transonic aerodynamics Missile configurations Pilotless aircraft		18. Distribution Statement Unclassified - Unlimited	
19. Security Classif. (of this report) Unclassified	20. Security Classif. (of this page) Unclassified	21. No. of Pages 40	22. Price* \$3.00

# AERODYNAMIC CHARACTERISTICS OF A SWEEP-WING CRUISE MISSILE

AT MACH NUMBERS FROM 0.50 TO 2.86

By M. Leroy Spearman and Ida K. Collins  
Langley Research Center

## SUMMARY

An investigation has been made in the Mach number range from 0.50 to 2.86 to determine the longitudinal and lateral aerodynamic characteristics of a cruise missile having a  $58^\circ$  swept wing and conventional aft tails.

The results indicated a relatively high drag-rise Mach number of about 0.95. In addition, at this Mach number the basic configuration with zero control deflection could be trimmed near the lift coefficient required for maximum lift-drag ratio with a slightly positive static stability margin. The configuration indicated positive directional stability and positive effective dihedral throughout the normal operating cruise range.

## INTRODUCTION

In order to provide aerodynamic data suitable for preliminary design and performance evaluation purposes, the NASA Langley Research Center has conducted a wind-tunnel study of a model representative of a cruise missile. This type of vehicle might be applicable to missions such as surface- or air-launched tactical or strategic missiles, unmanned reconnaissance, or countermeasure decoys. The model had a wing with  $58^\circ$  of leading-edge sweep and conventional aft tail surfaces with  $63^\circ$  of leading-edge sweep.

## COEFFICIENTS AND SYMBOLS

The moment reference point is at a longitudinal station corresponding to 48 percent of the wing mean aerodynamic chord.

The coefficients and symbols are defined as follows:

- A            cross-sectional-area parameter
- b            wing span, 56.39 cm (22.20 in.)

$C_D$	drag coefficient, $\frac{\text{Drag}}{qS}$
$C_{D,0}$	drag coefficient at zero lift
$C_L$	lift coefficient, $\frac{\text{Lift}}{qS}$
$C_{L\alpha}$	slope of lift curve, $\frac{\partial C_L}{\partial \alpha}$ , per deg
$C_l$	rolling-moment coefficient, $\frac{\text{Rolling moment}}{qSb}$
$C_{l\beta}$	effective-dihedral parameter, per deg
$C_m$	pitching-moment coefficient, $\frac{\text{Pitching moment}}{qS\bar{c}}$
$C_n$	yawing-moment coefficient, $\frac{\text{Yawing moment}}{qSb}$
$C_{n\beta}$	directional stability parameter, per deg
$C_Y$	side-force coefficient, $\frac{\text{Side force}}{qS}$
$C_{Y\beta}$	side-force parameter, per deg
$\bar{c}$	wing mean aerodynamic chord, 24.64 cm (9.70 in.)
L/D	lift-drag ratio (subscript max denotes maximum value)
M	free-stream Mach number
q	free-stream dynamic pressure
S	wing area, 1300 sq cm (201.5 sq in.)
x/l	body station in body lengths
$\alpha$	angle of attack, deg
$\beta$	angle of sideslip, deg

## APPARATUS AND TESTS

### Tunnel

Transonic tests were conducted in the Langley 8-foot transonic pressure tunnel. This is a variable-pressure, continuous-flow tunnel with a 2.44-meter-square (8-ft) test section and a Mach number range of 0.20 to 1.30. Supersonic tests were made in the low Mach number leg of the Langley Unitary Plan wind tunnel. This is also a variable-pressure, continuous-flow facility with a 1.22-meter-square (4-ft) test section and an asymmetric sliding-block nozzle, which provides a Mach number range from 1.47 to 2.86.

### Model

A three-view drawing of the model is shown in figure 1, and some geometric characteristics are given in table I. A photograph of the model is presented in figure 2. The wing section was a NACA 65A006 in the stream direction, and the wing had  $5^\circ$  of negative dihedral. The horizontal and vertical tails also had NACA 65A006 sections in the stream direction. No provisions were made for airflow through the model or for control-surface deflection. The basic body cross sections were circular, and a simulated equipment fairing was attached along the center line on the underside of the body.

### Tests

The tests were conducted at a constant Reynolds number of  $8.202 \times 10^6$  per meter ( $2.5 \times 10^6$  per foot).

The dewpoint was maintained low enough to insure negligible condensation effects. In order to insure boundary-layer transition to turbulent conditions, 0.159-cm-wide (0.0625-in.) strips of No. 120 carborundum grit were placed on the wing and tails 1.02 cm (0.4 in.) behind the leading edges (measured streamwise) and on the body 3.05 cm (1.2 in.) aft of the nose. The angle of attack was varied at sideslip angles of about  $0^\circ$ ,  $2^\circ$ , and  $5^\circ$  at Mach numbers from 0.50 to 1.20. Tests were made at angle of attack at Mach numbers of 2.00, 2.50, and 2.86 for sideslip angles of about  $0^\circ$  and  $3^\circ$ .

### Measurements

Aerodynamic forces and moments on the model were measured by means of a six-component electrical strain-gage balance, which was housed within the model. The balance was attached to a sting, which, in turn, was rigidly fastened to the tunnel support system. Balance-chamber pressure was measured by means of a single static-pressure orifice located in the vicinity of the balance.

## Corrections and Accuracy

The angle of attack has been corrected for deflection of the balance and sting due to aerodynamic loads, as well as for tunnel airflow misalignment. The drag results have been adjusted to correspond to free-stream static pressure acting over the model base.

## PRESENTATION OF RESULTS

In the graphical presentation, the longitudinal results are referred to the stability-axis system, and the lateral results are referred to the body-axis system. The moment reference is on the body center line at a point corresponding to 48 percent  $\bar{c}$ . The graphical results are presented in the following figures:

	Figure
Longitudinal aerodynamic characteristics . . . . .	3
Summary of longitudinal characteristics . . . . .	4
Transonic sideslip characteristics . . . . .	5
Supersonic sideslip derivatives . . . . .	6

## DISCUSSION

### Longitudinal Aerodynamic Characteristics

The longitudinal aerodynamic characteristics at each Mach number are presented in figure 3 and are summarized in figure 4. The pitching-moment characteristics are generally linear over the positive lift-coefficient range up to approximately  $(L/D)_{\max}$ , and then a pitch-down tendency occurs. Nonlinearities in pitching moment above the lift coefficient for  $(L/D)_{\max}$  do not necessarily constitute a reason for concern for vehicles of this type, which, generally speaking, are not required to maneuver to high lifts and are not required to land.

The summary of longitudinal characteristics (fig. 4) indicates a relatively high drag-rise Mach number of about 0.95. This result is due in part to the high sweep angle of the wing and tails. In addition, the location of the tails should reduce the afterbody closure drag effects. The favorable drag characteristics can thus be attributed to the area distribution of the vehicle. As shown in figure 4(a), the normal area distribution is relatively smooth and symmetric about the midbody station. Such a shape is conducive to low transonic drag. The neutral-point location is essentially constant over the subsonic range at about 43 percent  $\bar{c}$ . The neutral point shifts rearward about 26 percent  $\bar{c}$  from subsonic speeds to  $M = 2.0$  and the maximum  $L/D$  decreases to about 3.5.

A positive increment of  $C_m$  occurs at  $C_L = 0$  which, for the proper center-of-gravity location, would make it possible to achieve trimmed conditions with zero control

deflection near the lift coefficient for  $(L/D)_{\max}$  with a slightly positive static margin. Results shown in figure 4(b) for  $M = 0.95$  indicate that a forward shift in center of gravity of only 4 percent  $\bar{c}$  would provide such a condition.

### Lateral Aerodynamic Characteristics

Because of the nonlinear lateral aerodynamic characteristics at transonic speeds, the variations of  $C_n$ ,  $C_l$ , and  $C_Y$  with angle of attack for sideslip angles of approximately  $0^\circ$ ,  $2^\circ$ , and  $5^\circ$  are shown in figure 5 for each transonic Mach number. The lateral characteristics were found to be linear for the supersonic tests. Sideslip derivatives measured between sideslip angles of  $0^\circ$  and about  $3^\circ$  were obtained and are shown in figure 6 as a function of  $\alpha$  for Mach numbers of 2.00, 2.50, and 2.86. These results, in general, indicate positive directional stability and a positive dihedral effect throughout the normal operating cruise range. It should be pointed out that the forward movement of the moment reference point required to provide longitudinal stability at subsonic speeds would also result in an increase in the positive value of directional stability at all Mach numbers.

### SUMMARY OF RESULTS

An investigation has been made in the Mach number range from 0.50 to 2.86 to determine the longitudinal and lateral aerodynamic characteristics of a cruise missile having a  $58^\circ$  swept wing and conventional aft tails. The results of the investigation are as follows:

1. The configuration had a relatively high drag-rise Mach number of about 0.95.
2. The configuration could be trimmed with zero control deflection near the lift coefficient required for maximum lift-drag ratio at a Mach number of 0.95.
3. The configuration had positive directional stability and positive effective dihedral throughout the normal operating cruise range.

Langley Research Center,  
National Aeronautics and Space Administration,  
Hampton, Va., October 4, 1972.

TABLE I.- GEOMETRIC CHARACTERISTICS

Forebody coordinates:

Body station		Radius	
cm	in.	cm	in.
0	0	0	0
.254	.100	.833	.328
.508	.200	1.179	.464
1.016	.400	1.661	.654
1.524	.600	2.027	.798
2.032	.800	2.324	.915
2.540	1.000	2.588	1.019
5.080	2.000	3.581	1.410
7.620	3.000	4.285	1.687
10.160	4.000	4.829	1.901
12.700	5.000	5.260	2.071
15.240	6.000	5.611	2.209
17.780	7.000	5.888	2.318
20.320	8.000	6.106	2.404
22.860	9.000	6.271	2.469
25.400	10.000	6.388	2.515
27.940	11.000	6.454	2.541
30.480	12.000	6.477	2.550

Afterbody:

Theoretical intersection of cylindrical centerbody and conical afterbody occurs at body station 83.2485 cm (32.775 in.). The transition region is faired with an arc of 50.800-cm (20.000-in.) radius.

Equipment fairing:

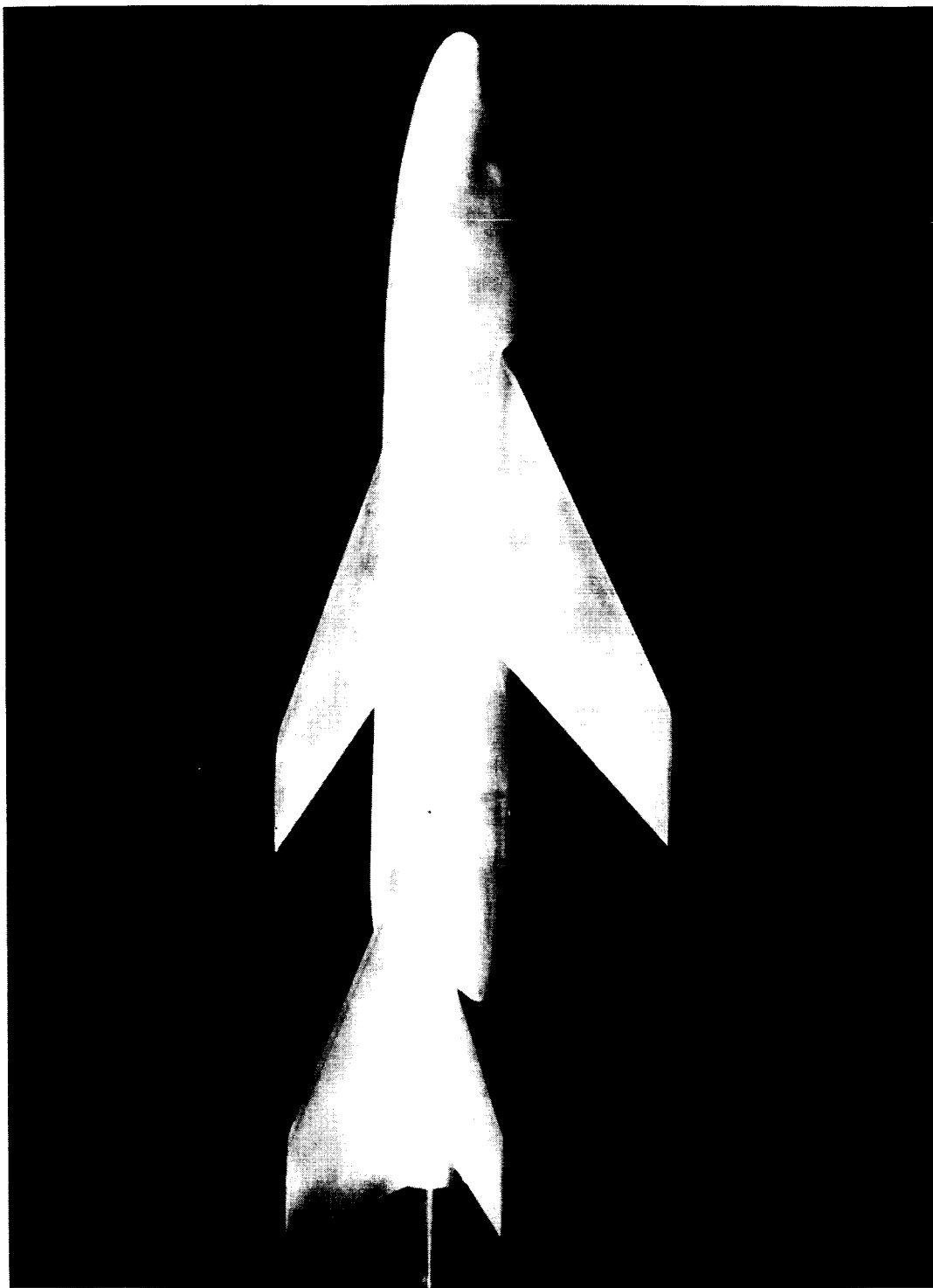
Constant depth of 1.905 cm (0.750 in.)

Forward contour faired with arc of 20.320-cm (8.000-in.) radius

Rear contour beveled 15°

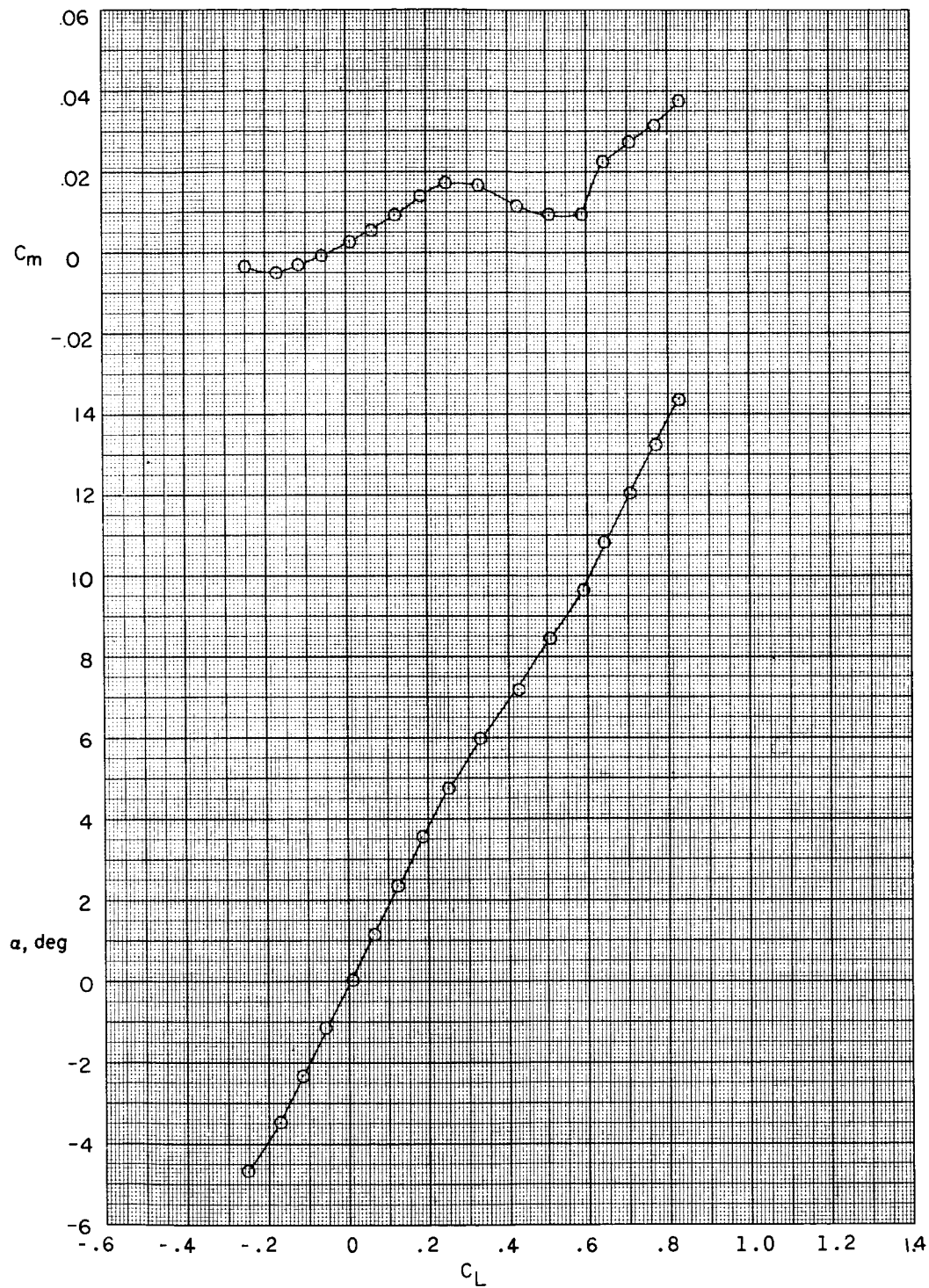






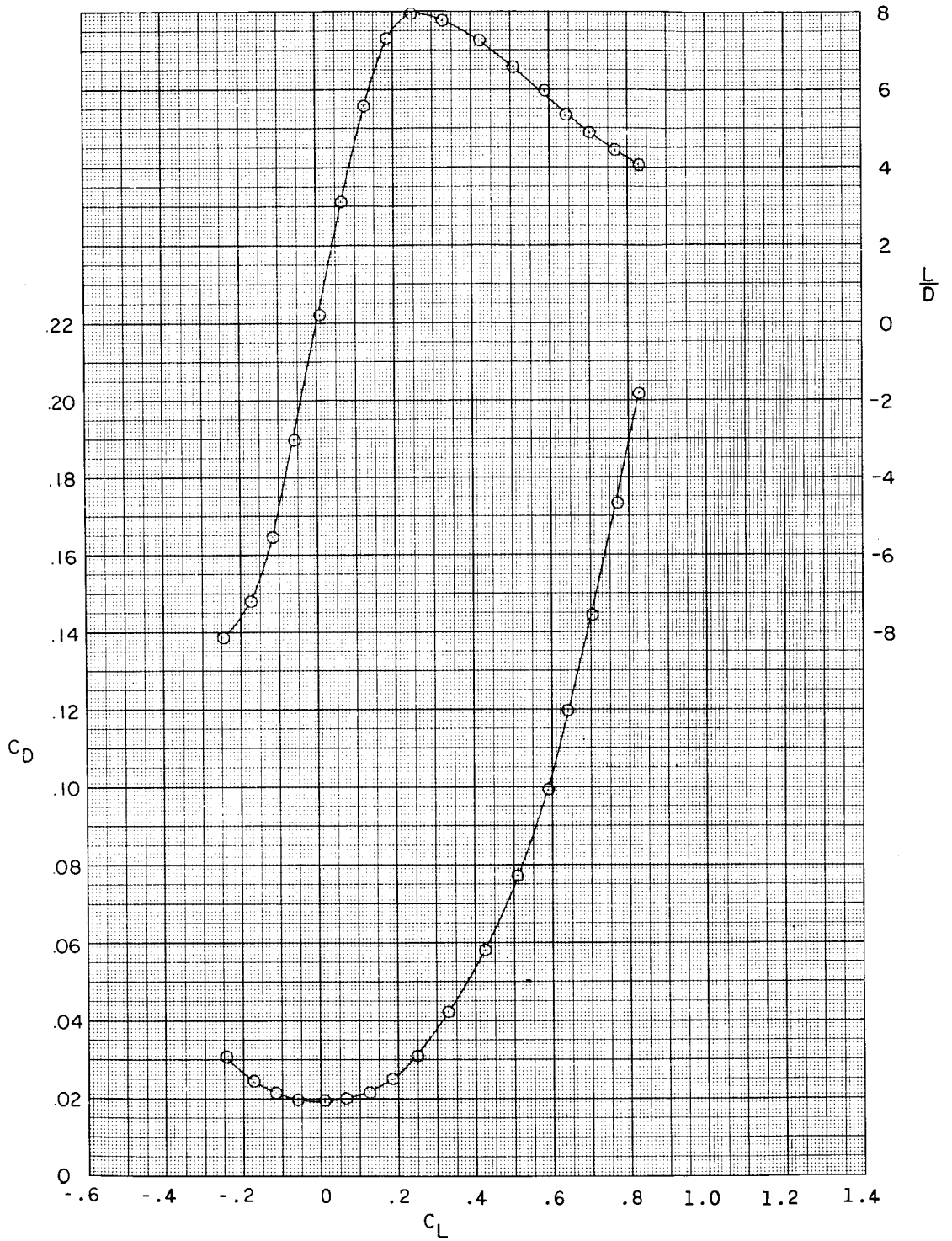
L-67-4691

Figure 2.- Photograph of model.



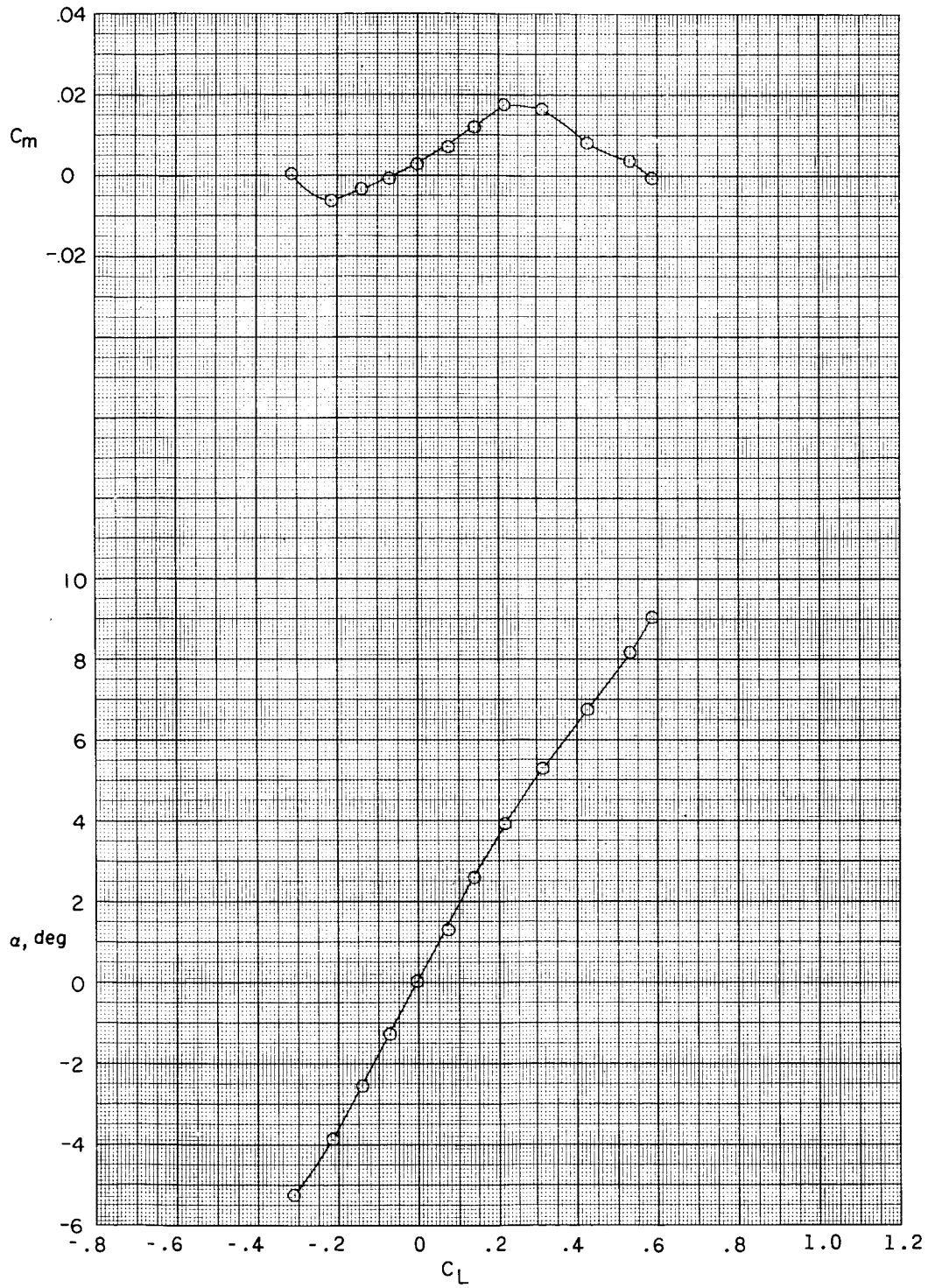
(a)  $M = 0.50$ .

Figure 3.- Longitudinal aerodynamic characteristics.



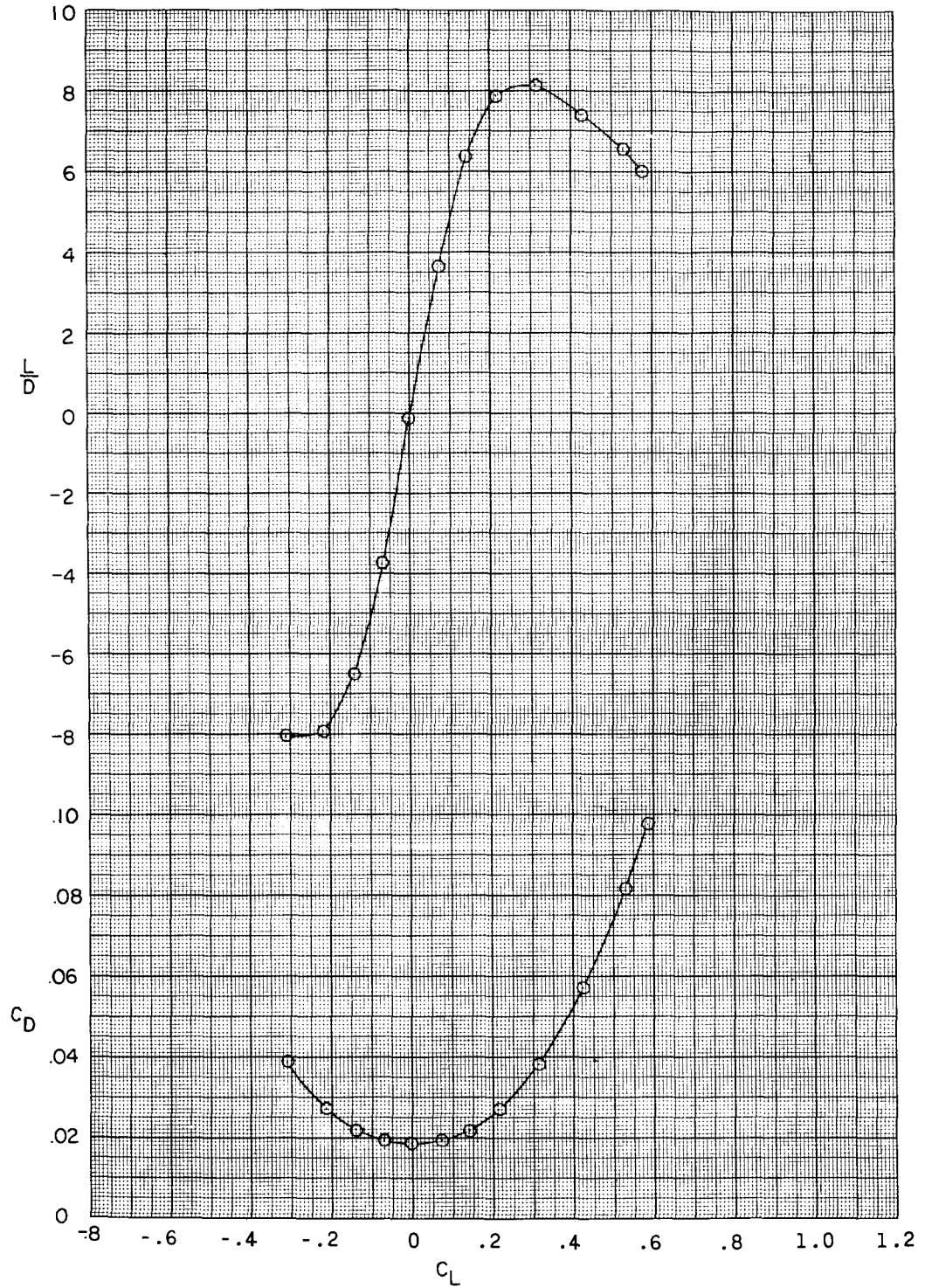
(a) Concluded.

Figure 3.- Continued.



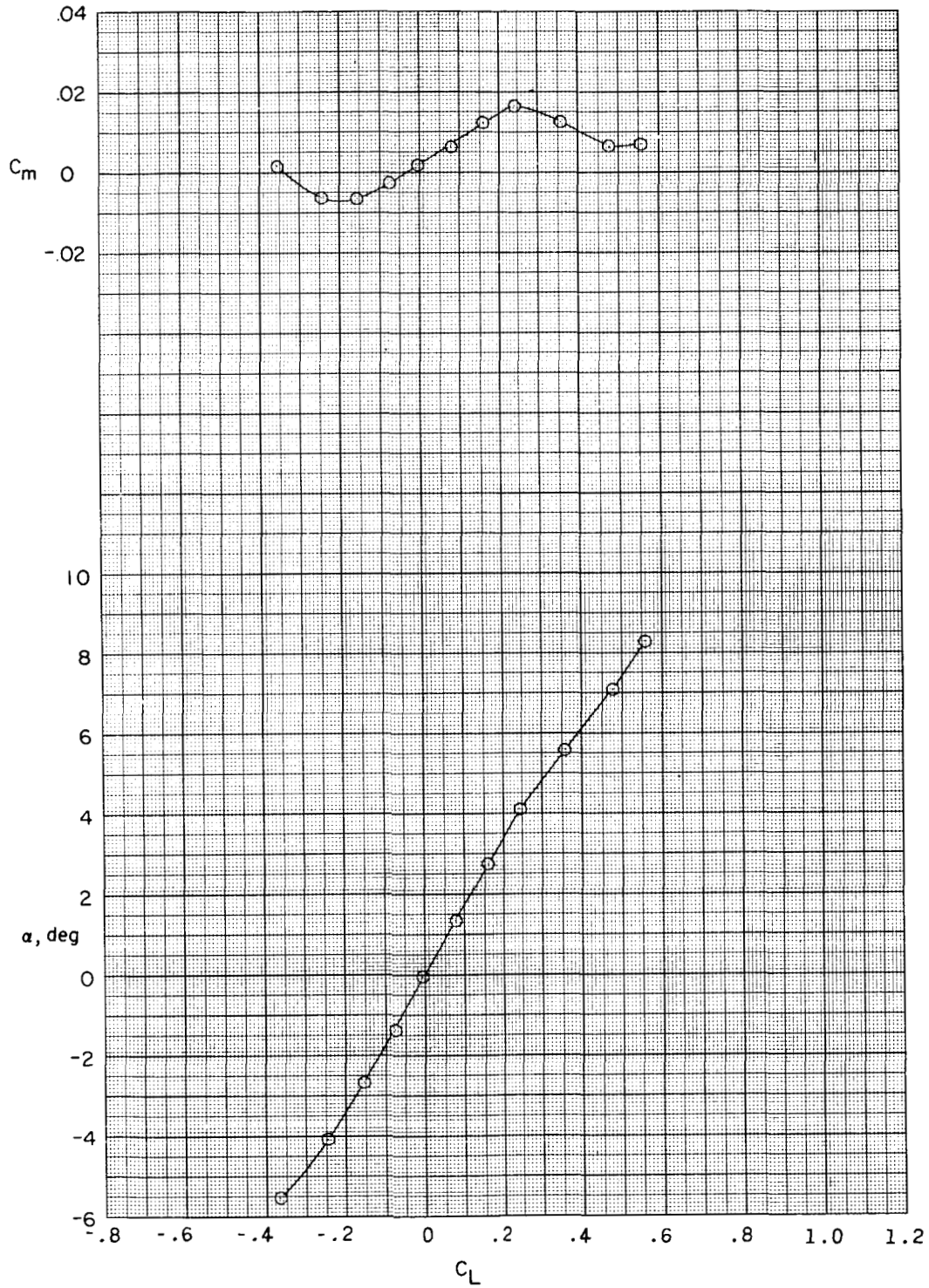
(b)  $M = 0.80$ .

Figure 3.- Continued.



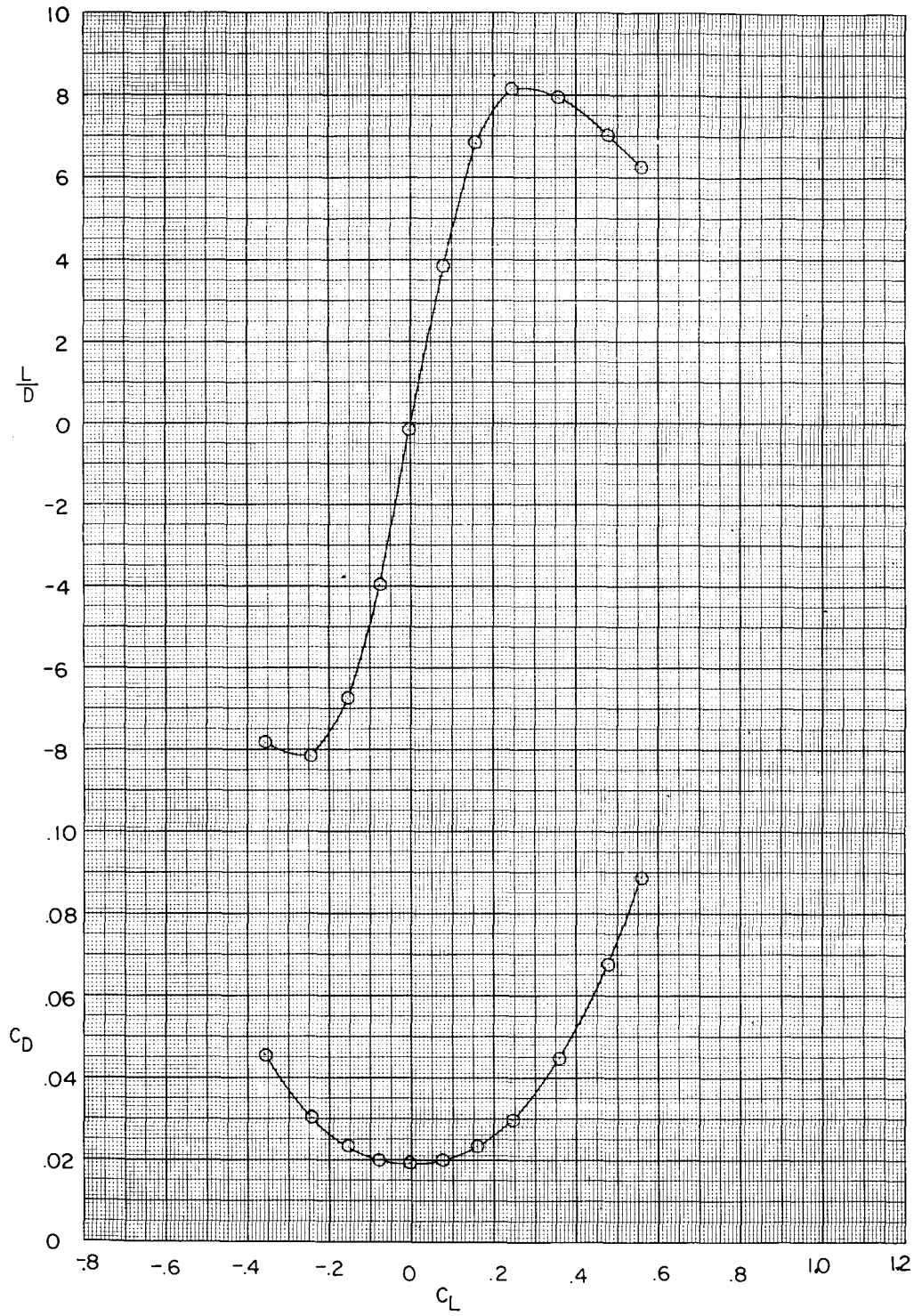
(b) Concluded.

Figure 3.- Continued.



(c)  $M = 0.90$ .

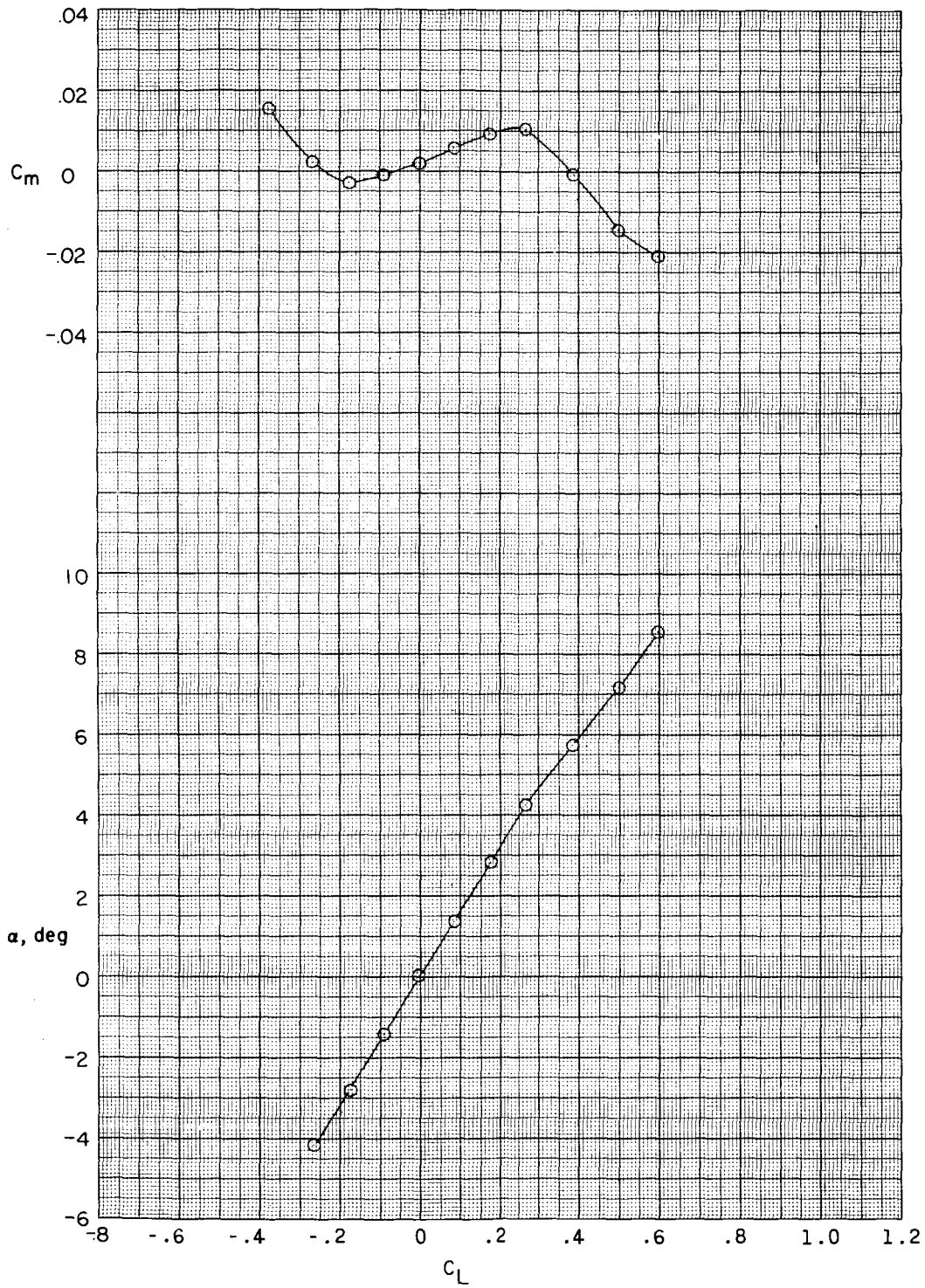
Figure 3.- Continued.



(c) Concluded.

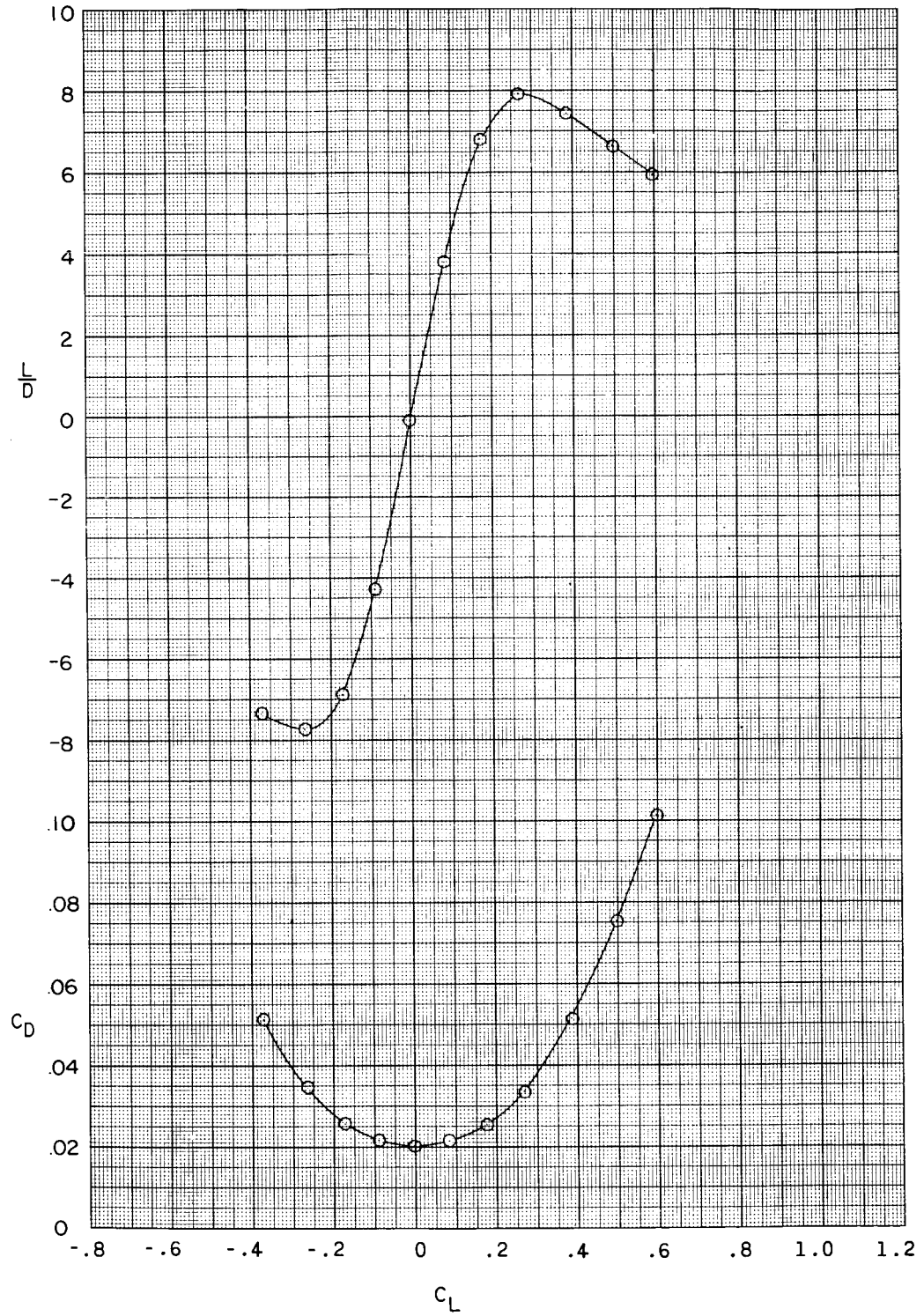
Figure 3.- Continued.





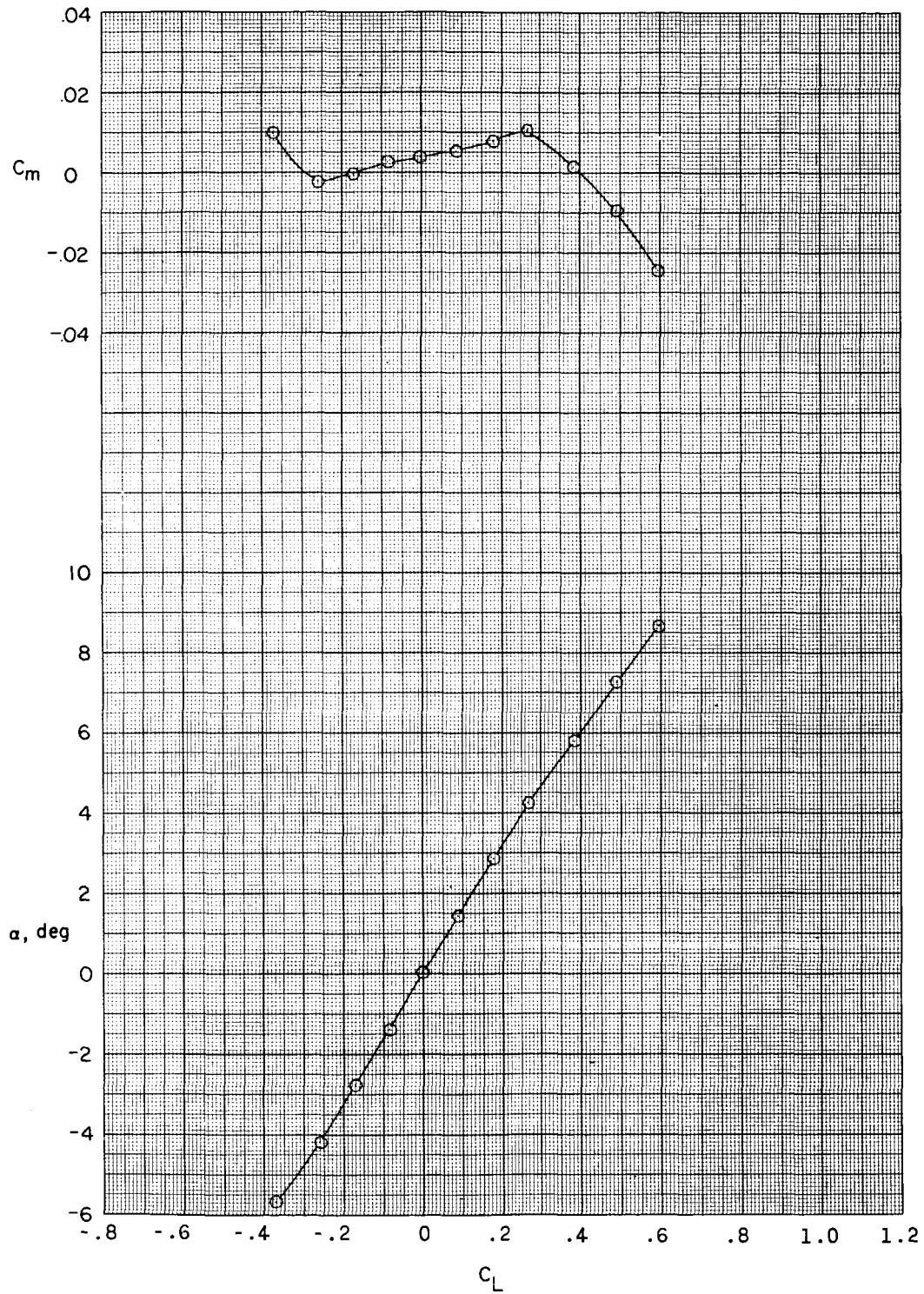
(d)  $M = 0.95$ .

Figure 3.- Continued.



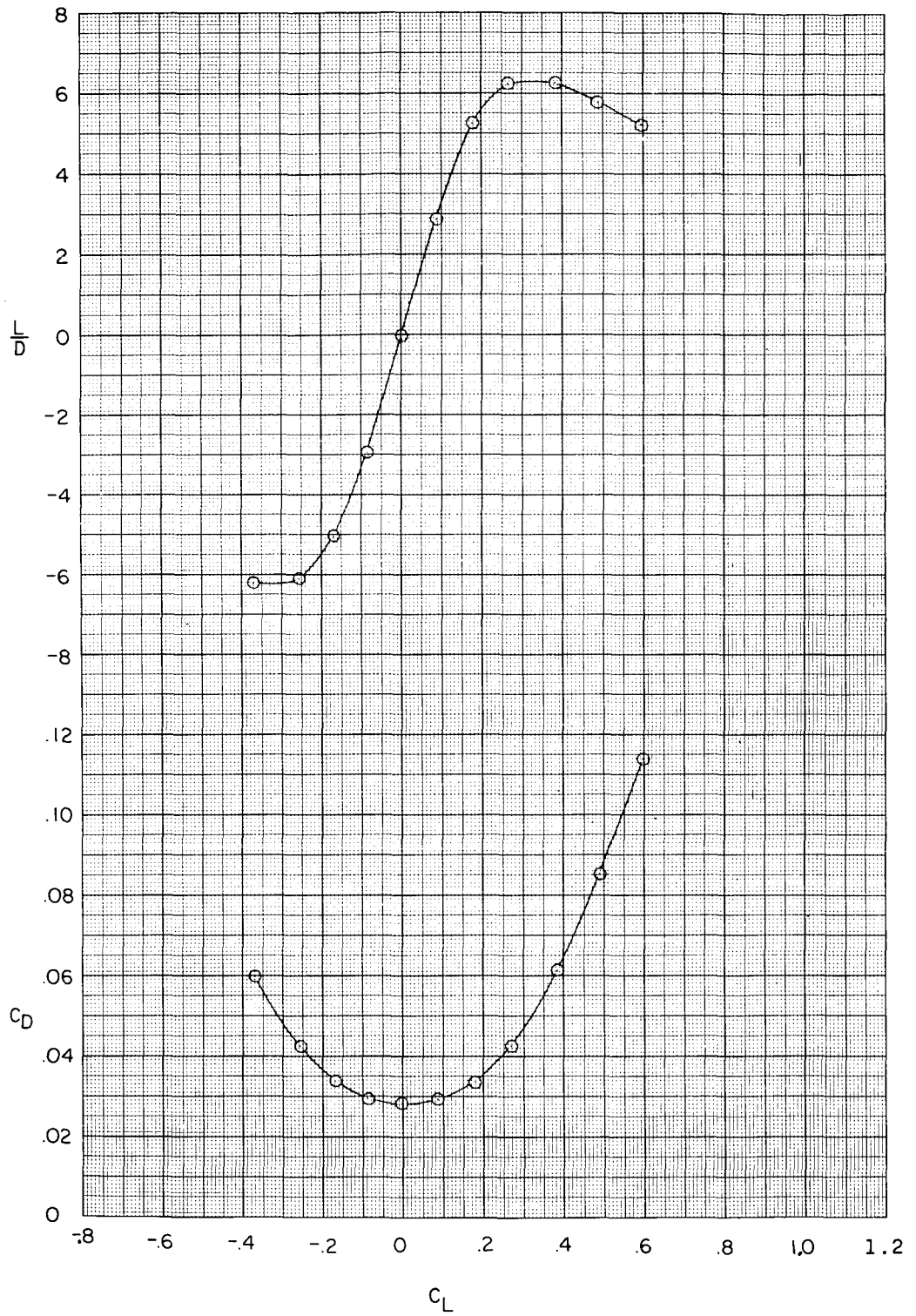
(d) Concluded.

Figure 3.- Continued.



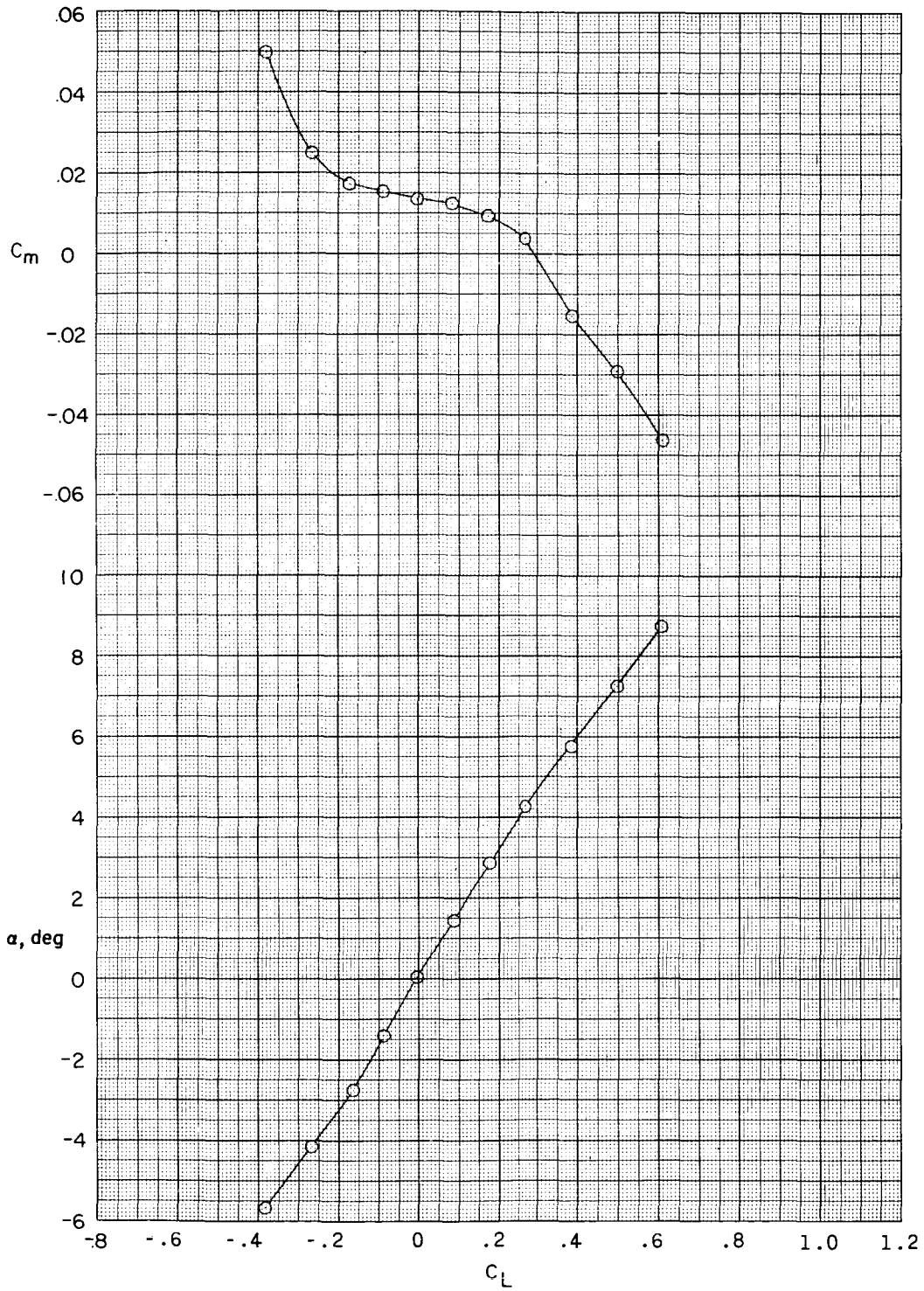
(e)  $M = 1.00$ .

Figure 3.- Continued.



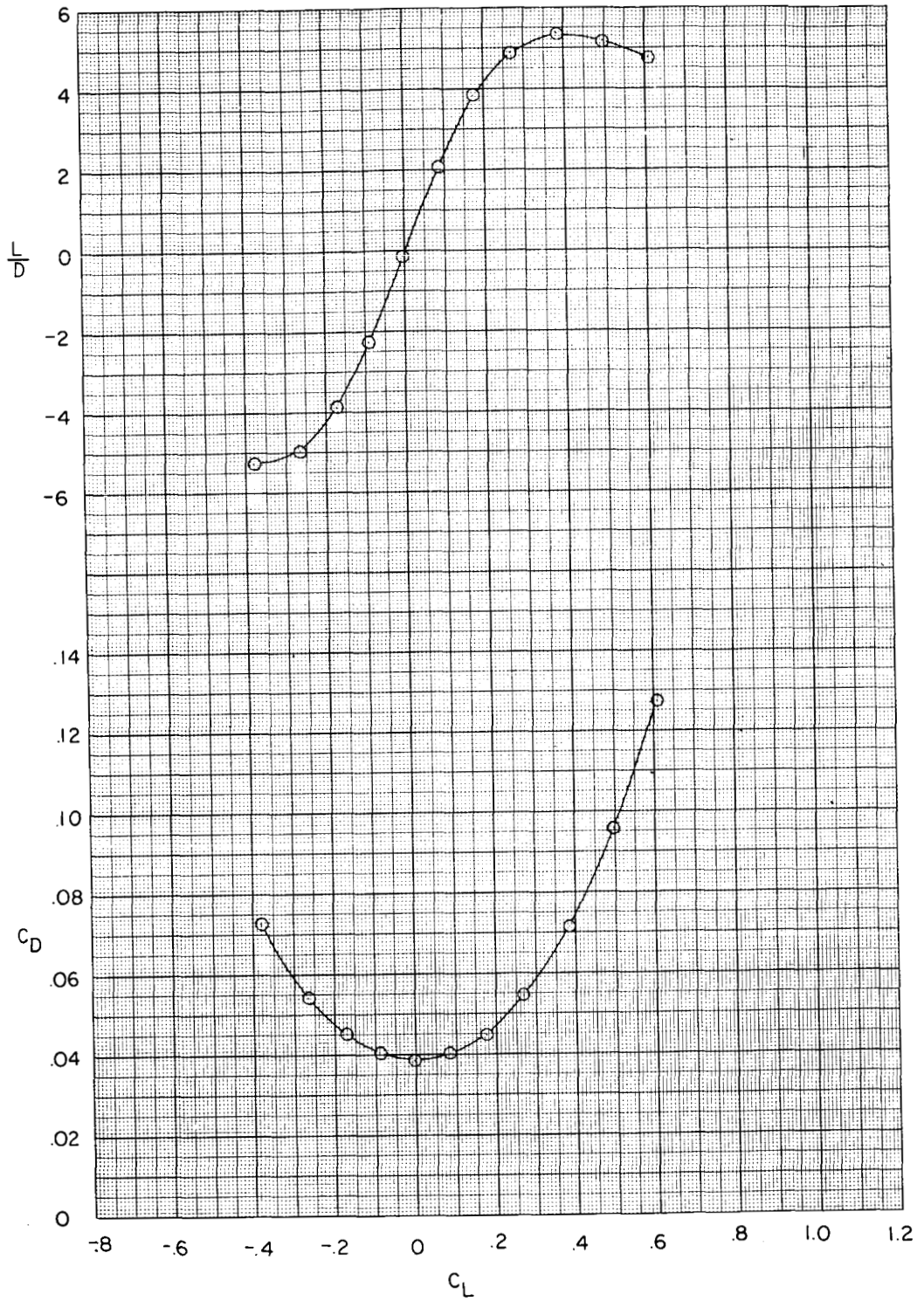
(e) Concluded.

Figure 3.- Continued.



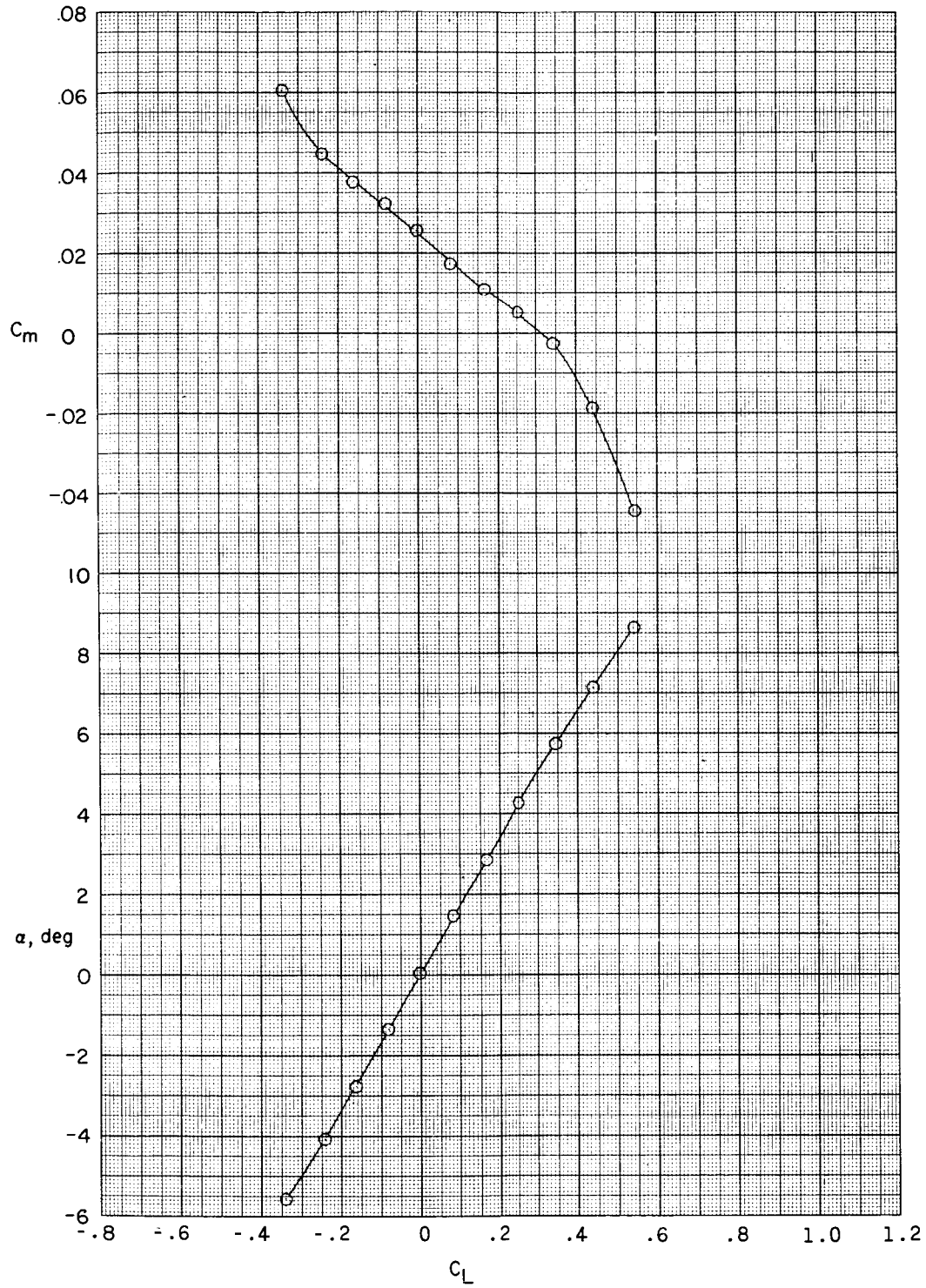
(f)  $M = 1.03$ .

Figure 3.- Continued.



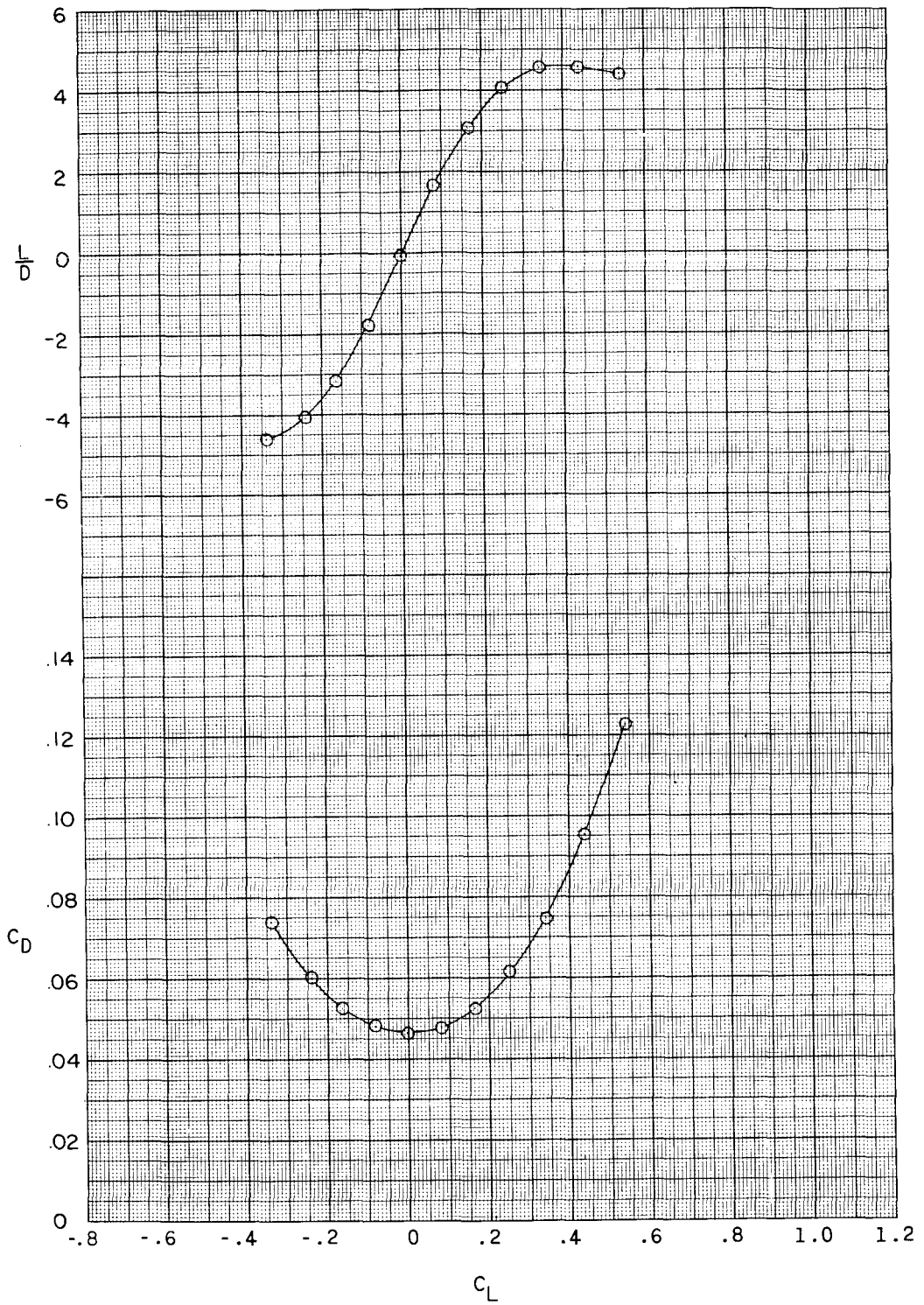
(f) Concluded.

Figure 3.- Continued.



(g)  $M = 1.20$ .

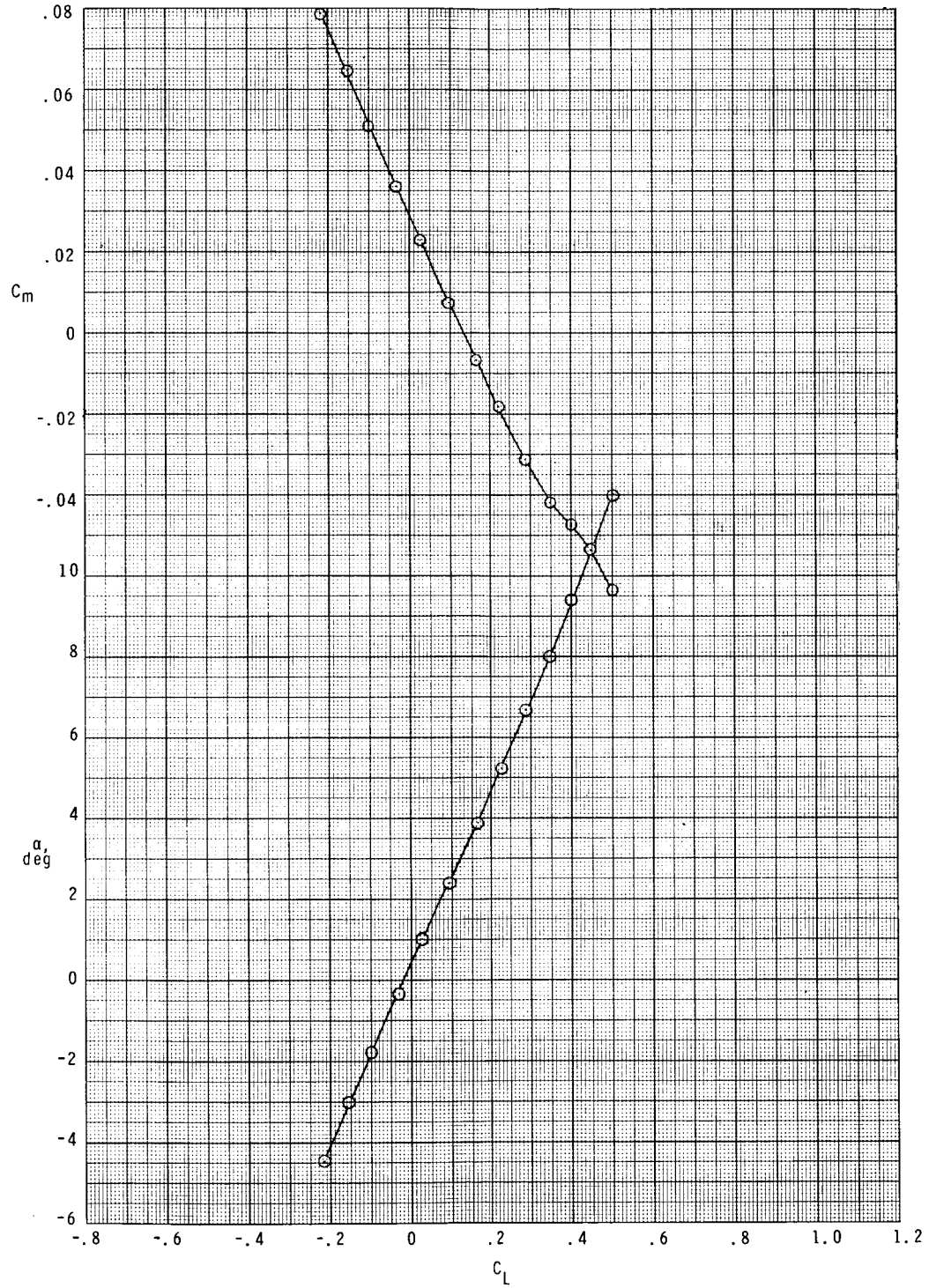
Figure 3.- Continued.



(g) Concluded.

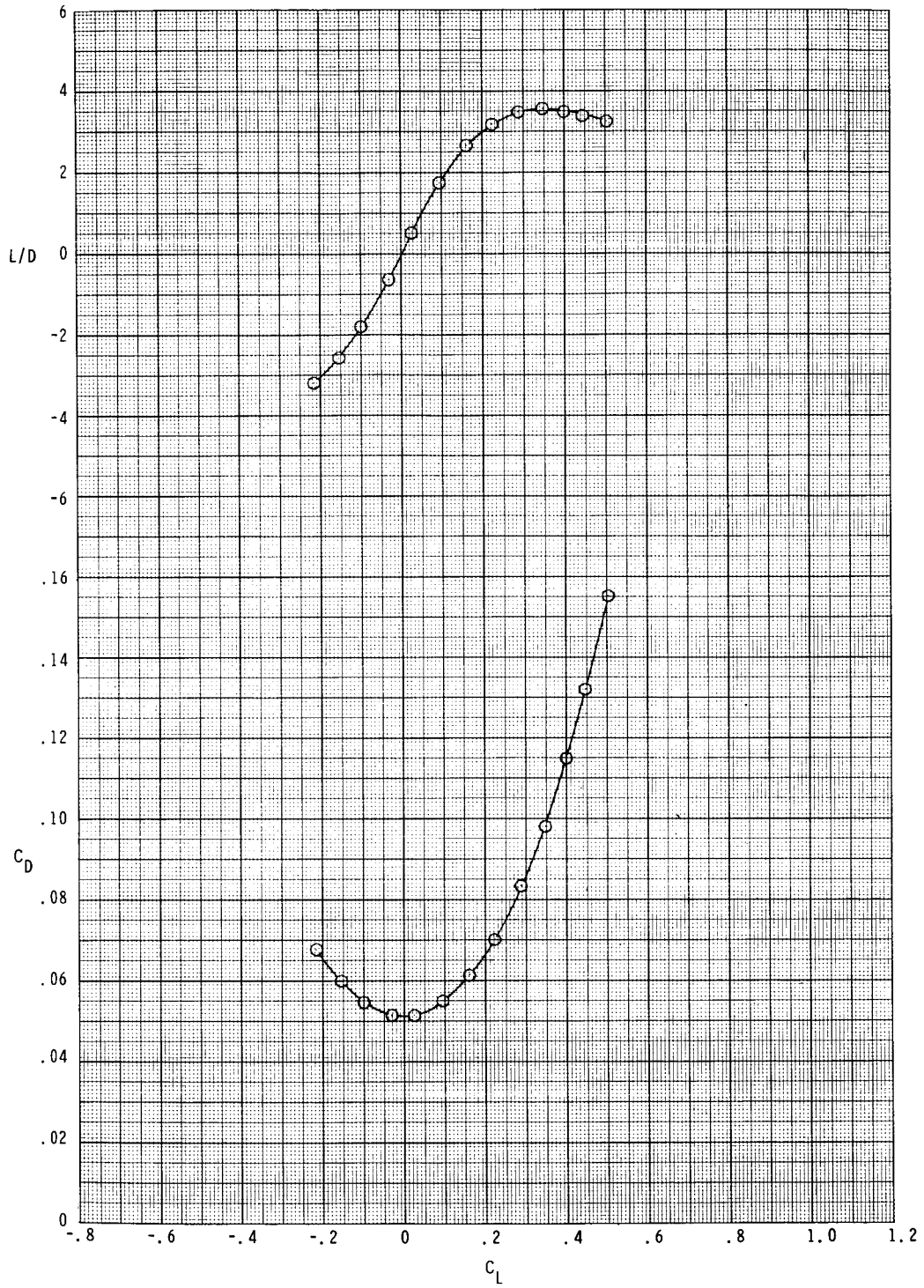
Figure 3.- Continued.





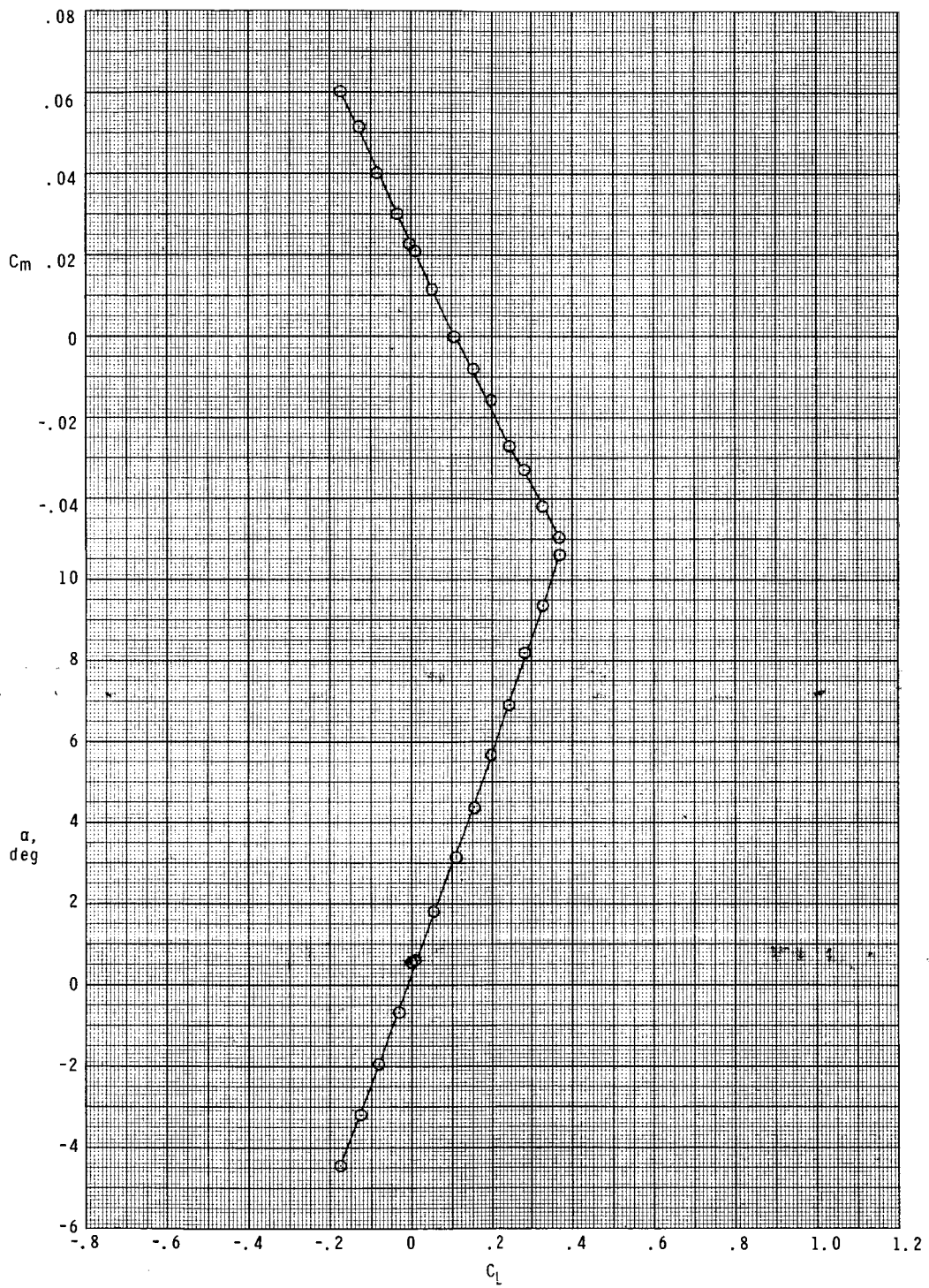
(h)  $M = 2.00$ .

Figure 3.- Continued.



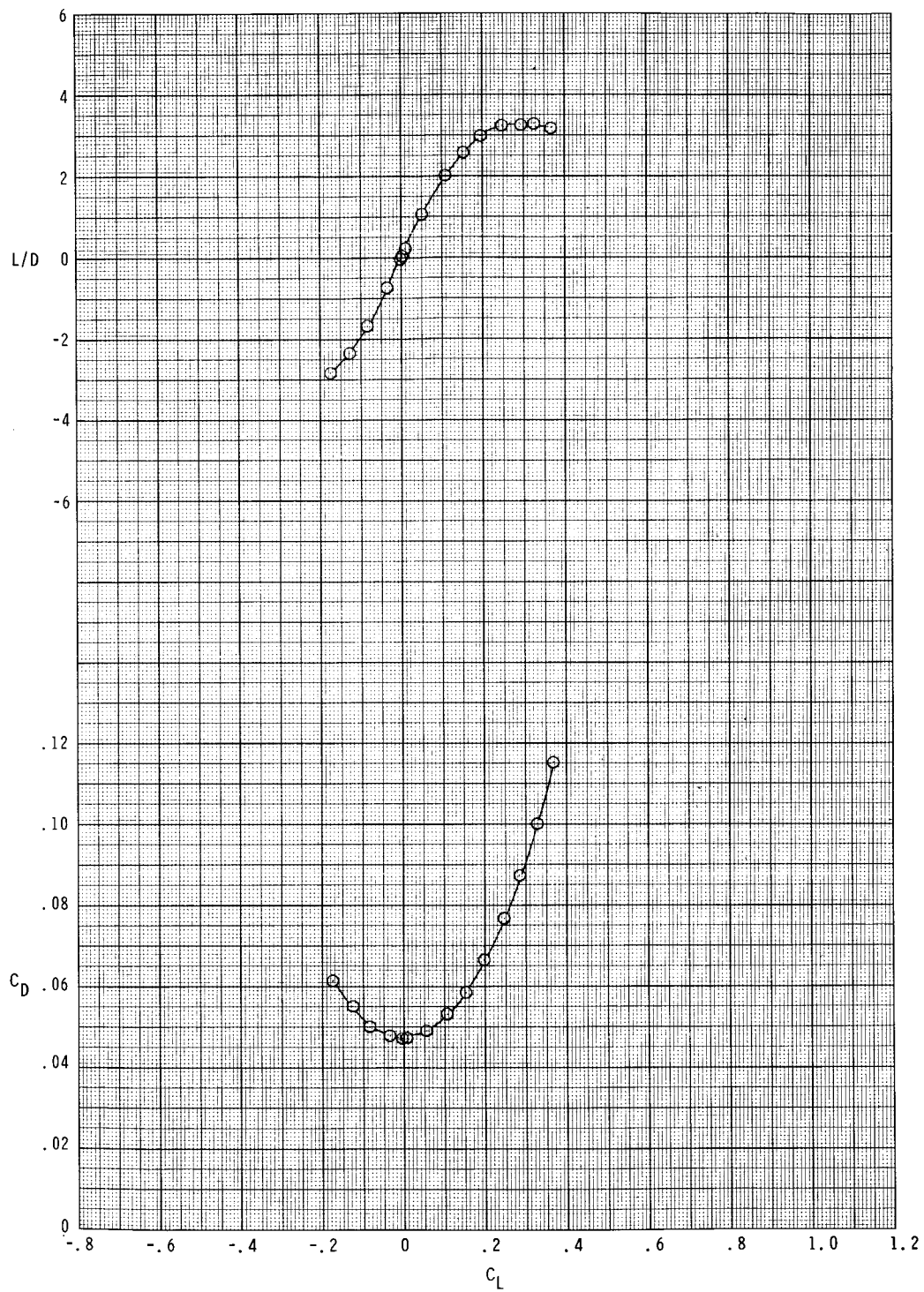
(h) Concluded.

Figure 3.- Continued.



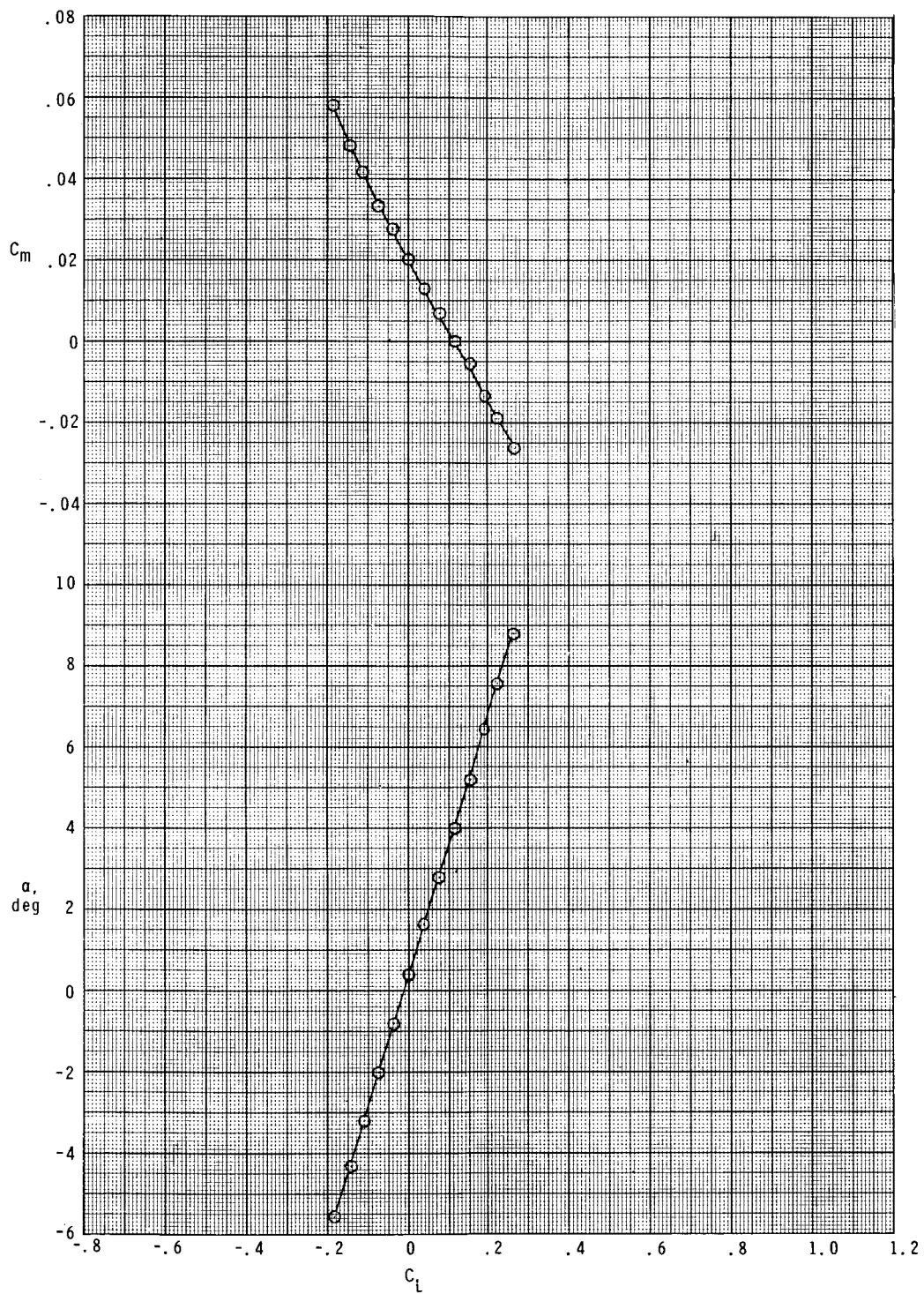
(i)  $M = 2.50$ .

Figure 3.- Continued.



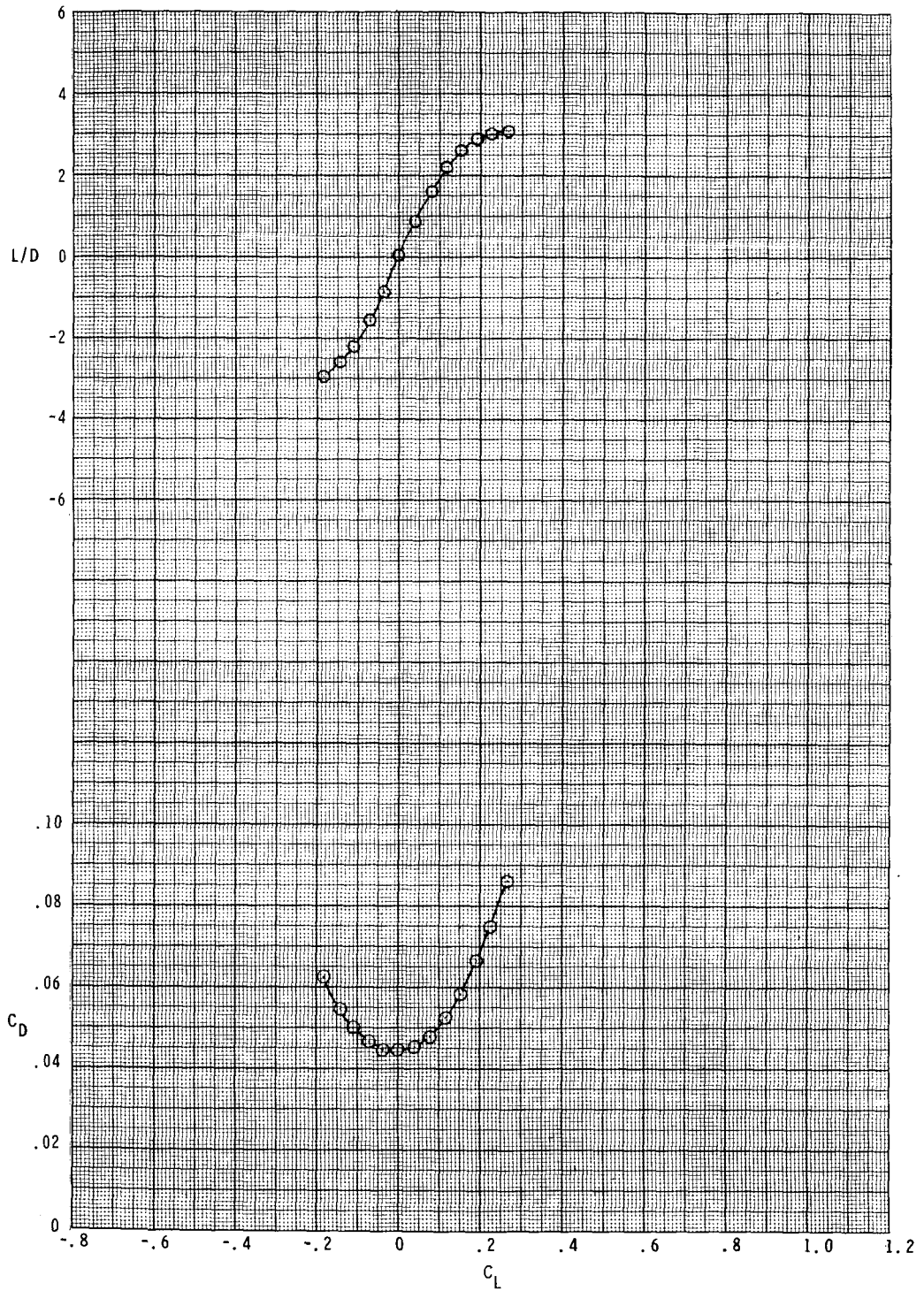
(i) Concluded.

Figure 3.- Continued.



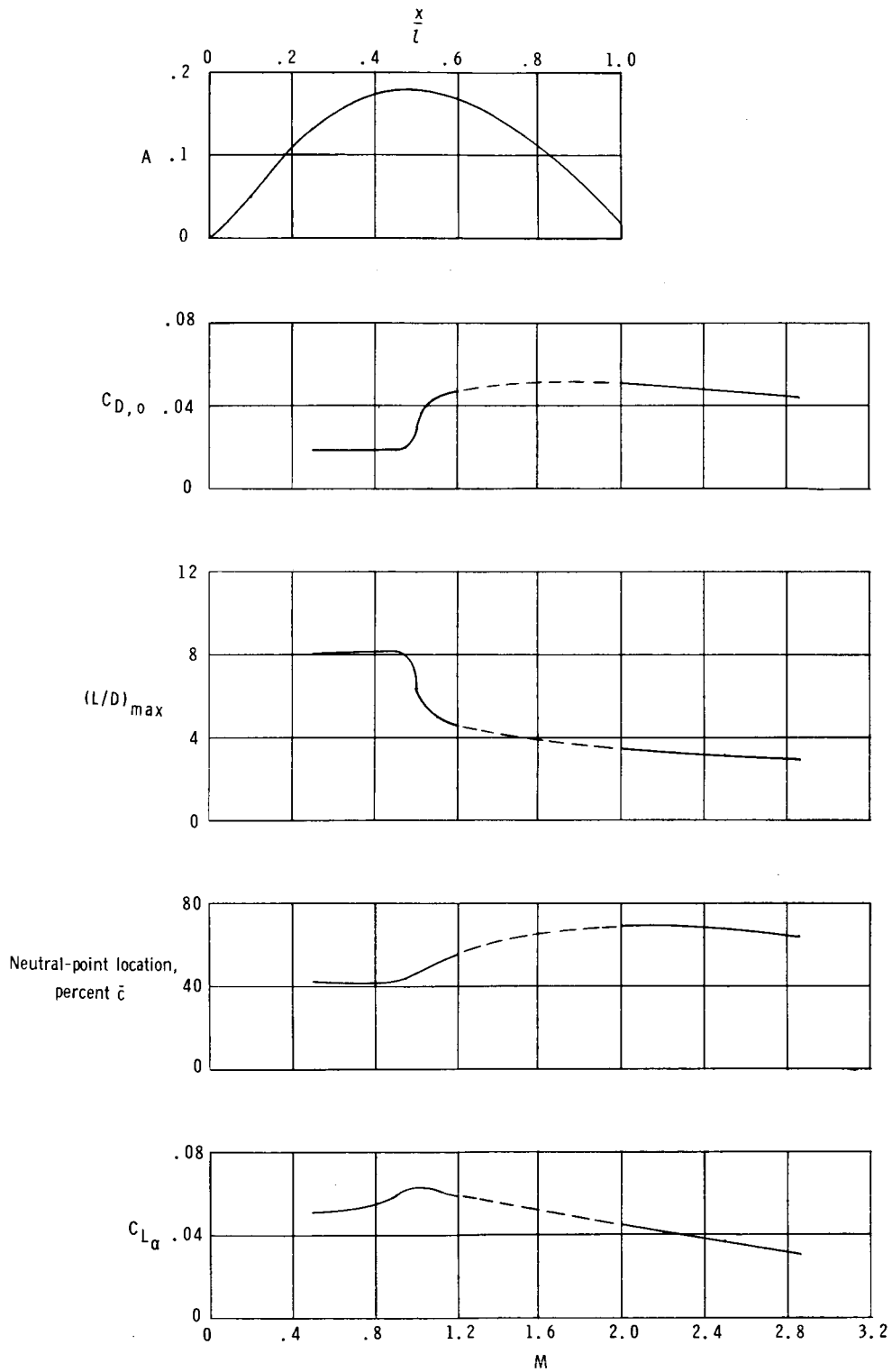
(j)  $M = 2.86$ .

Figure 3.- Continued.



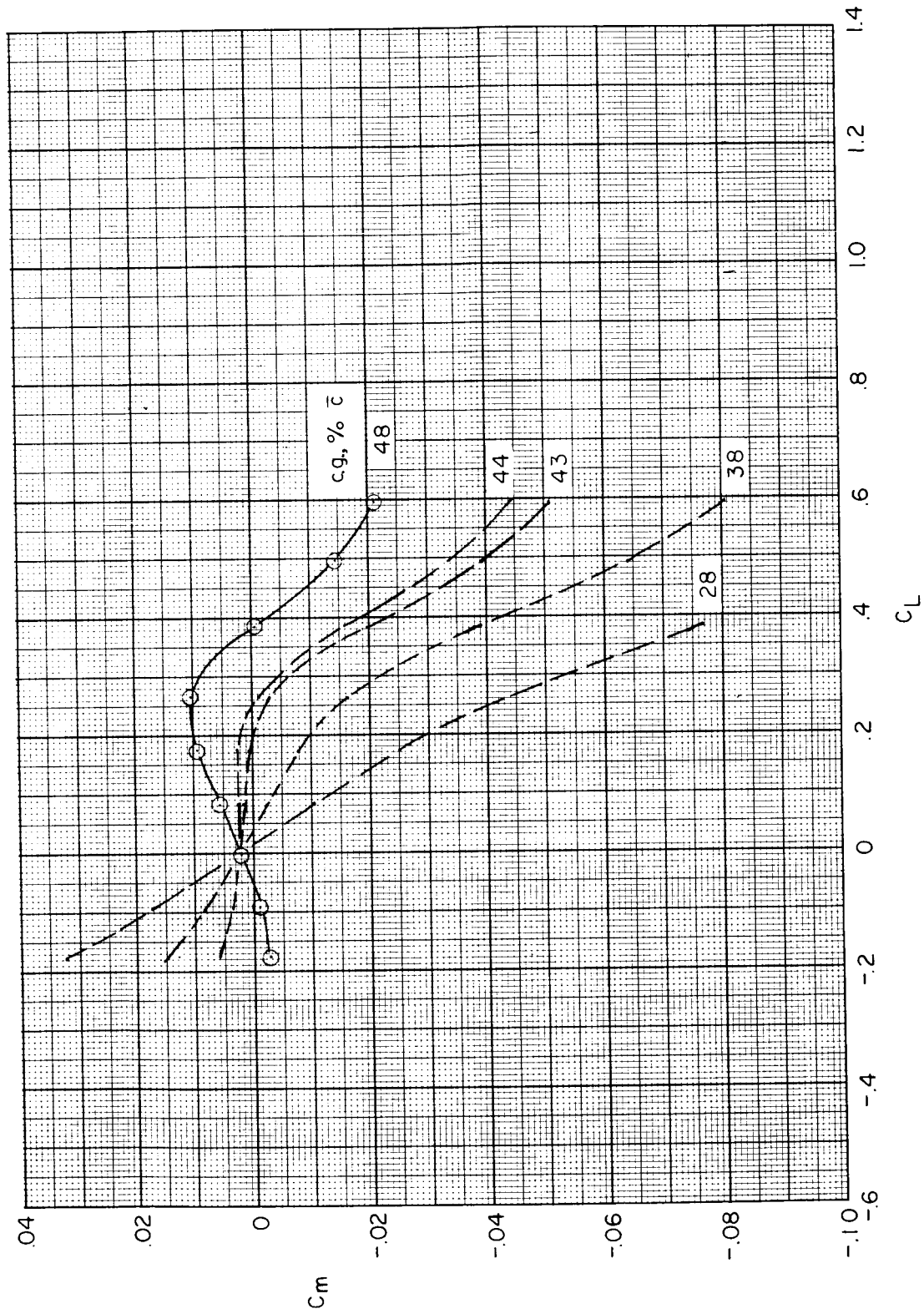
(j) Concluded.

Figure 3.- Concluded.



(a) Area distribution and various aerodynamic parameters.

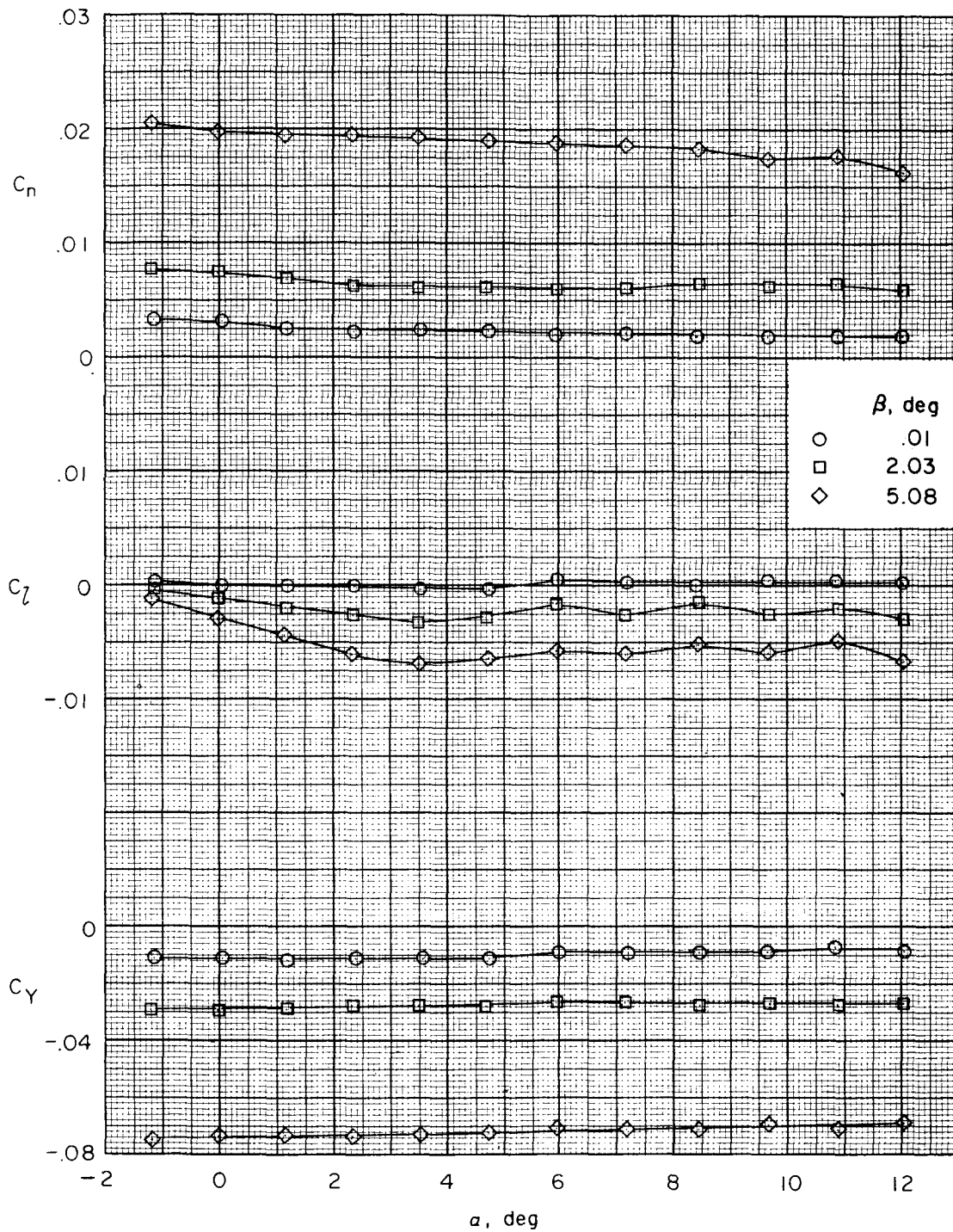
Figure 4.- Summary of longitudinal characteristics.



(b) Effect of center of gravity (c.g.) on longitudinal stability at  $M = 0.95$ .

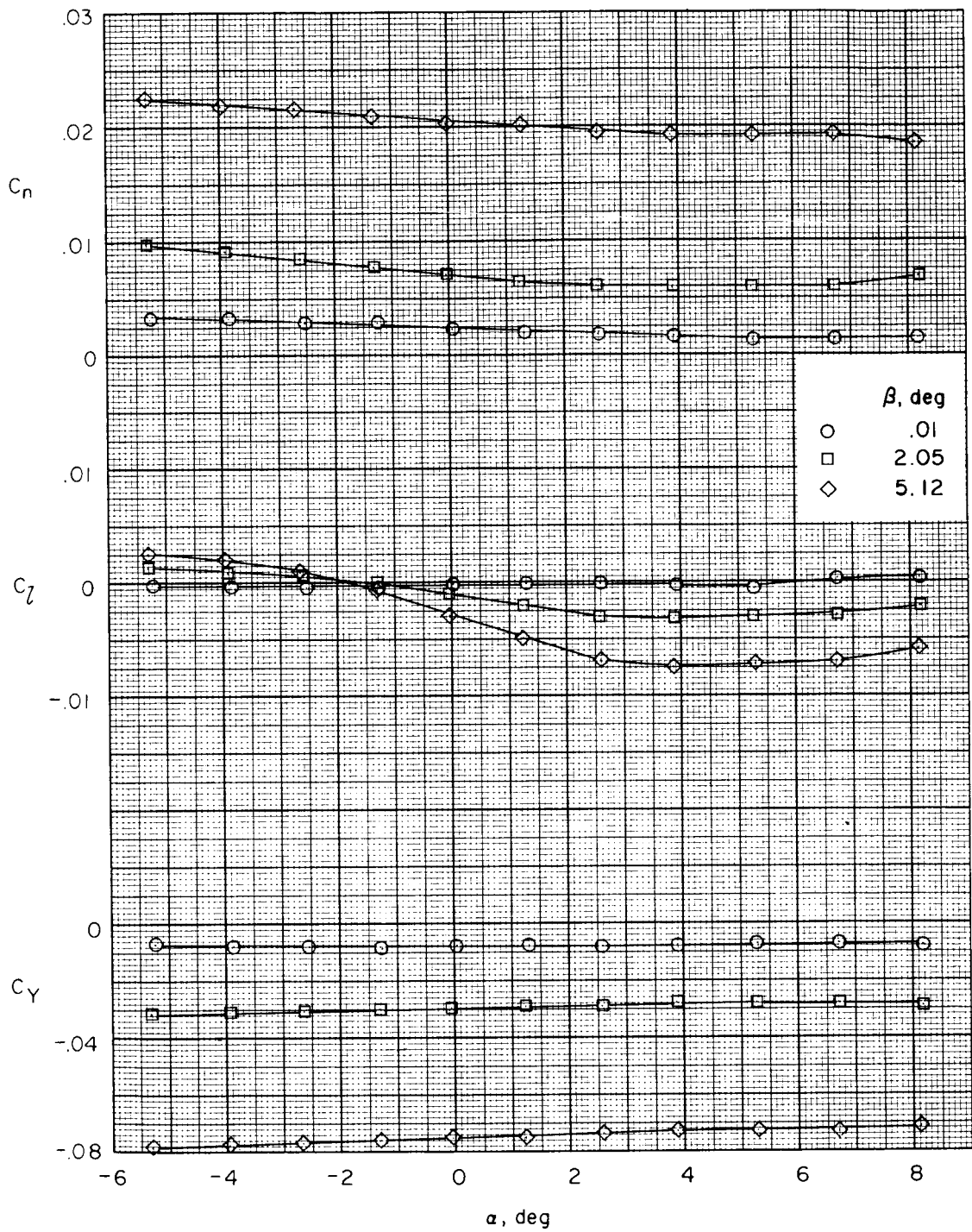
Figure 4. - Concluded.





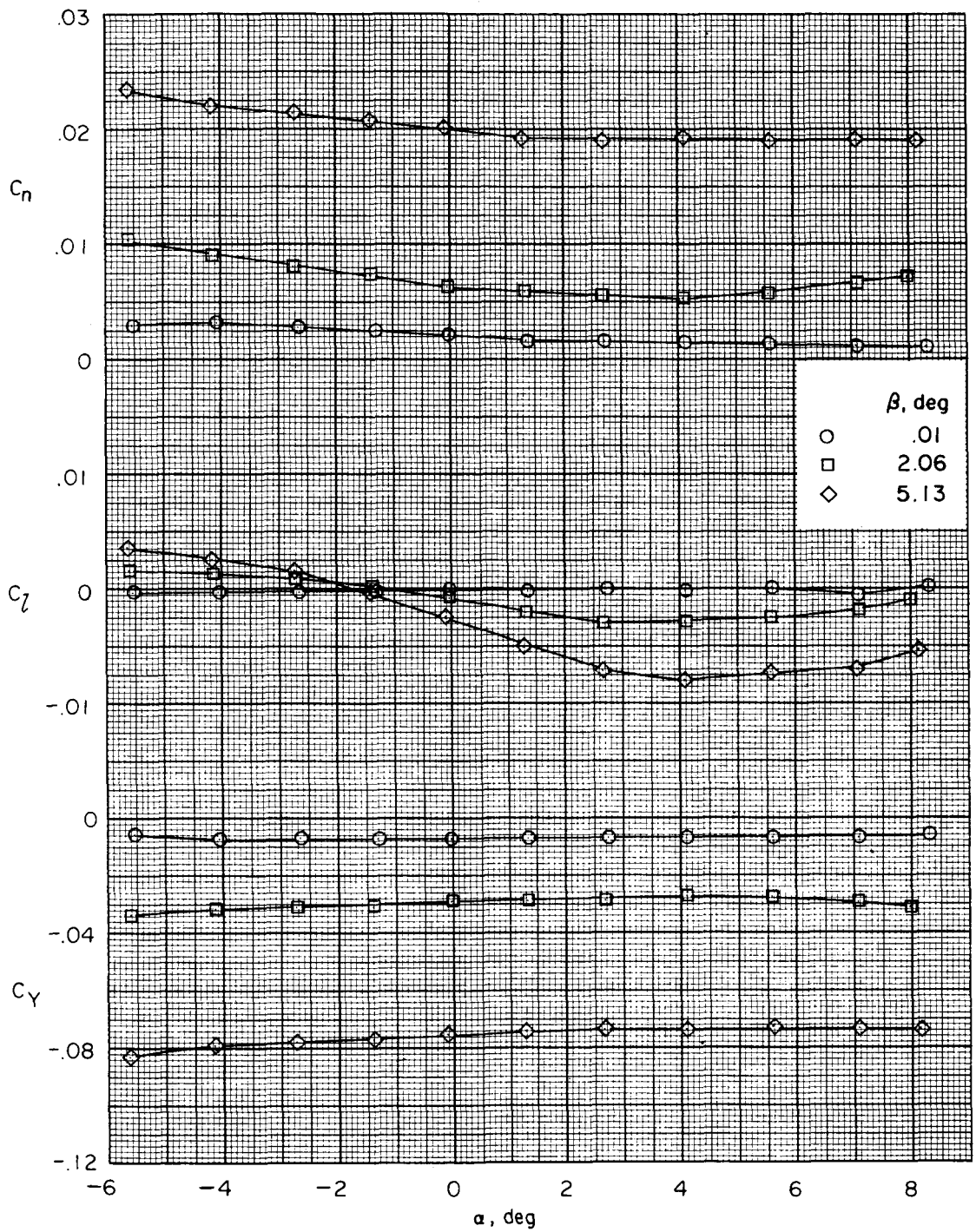
(a)  $M = 0.50$ .

Figure 5.- Transonic sideslip characteristics.



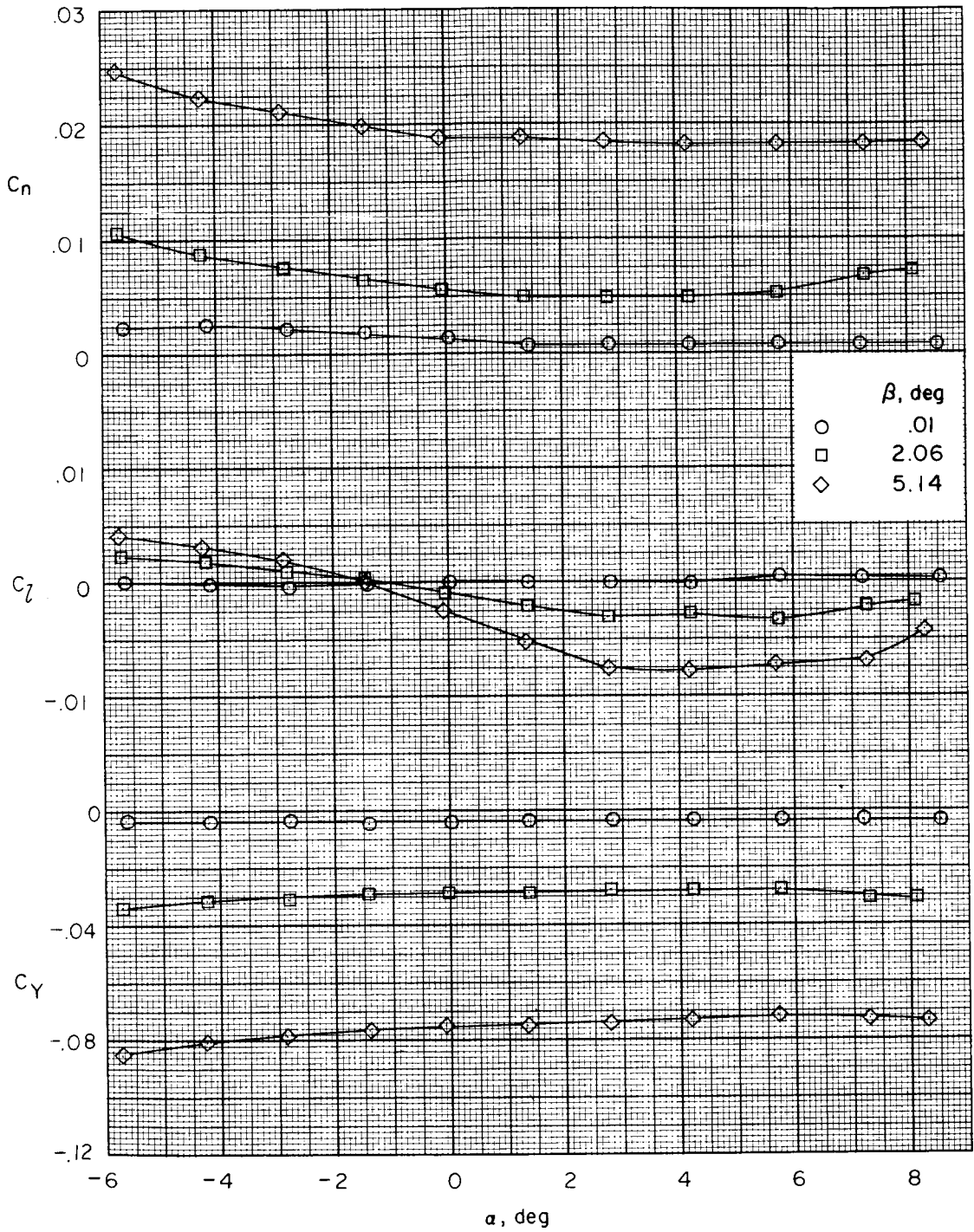
(b)  $M = 0.80$ .

Figure 5.- Continued.



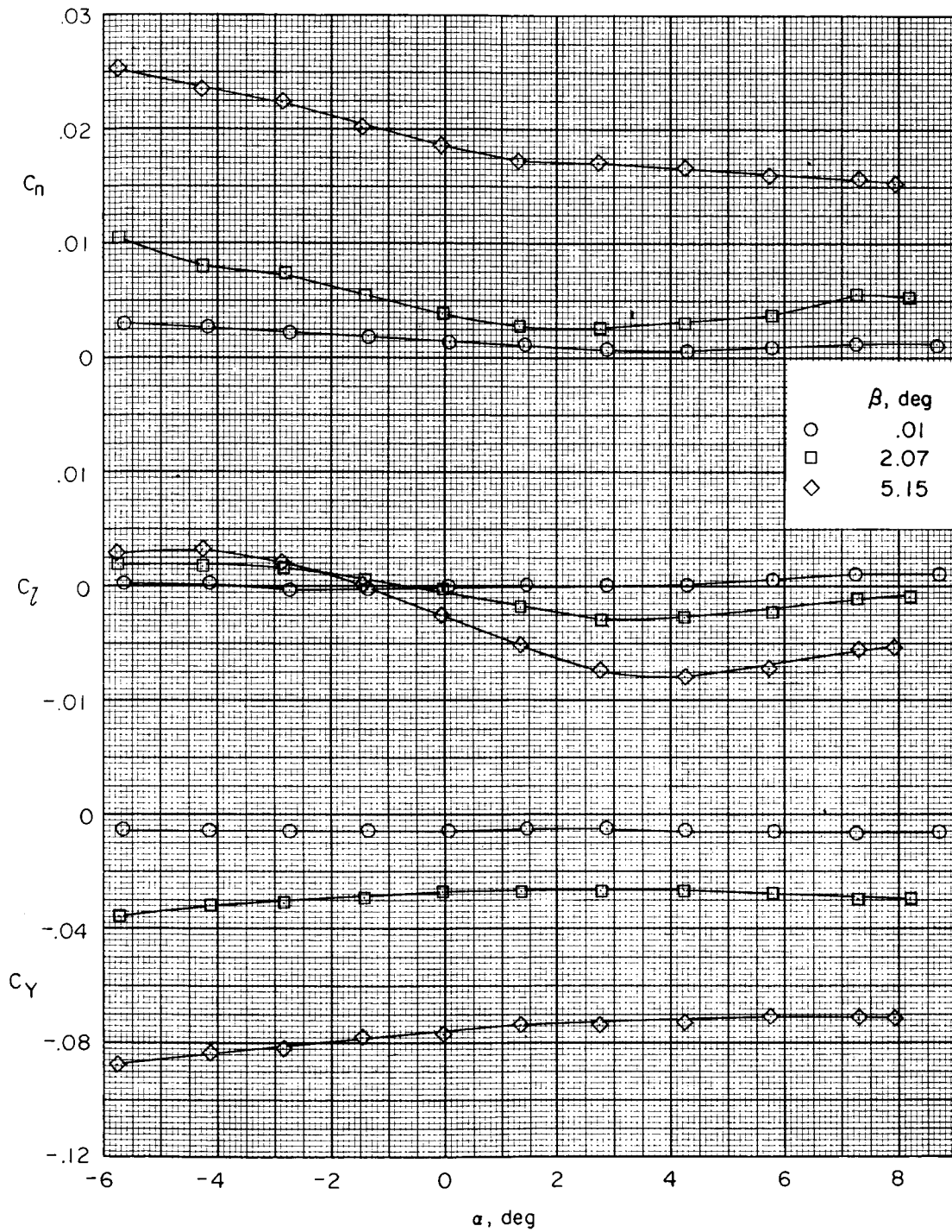
(c)  $M = 0.90$ .

Figure 5.- Continued.



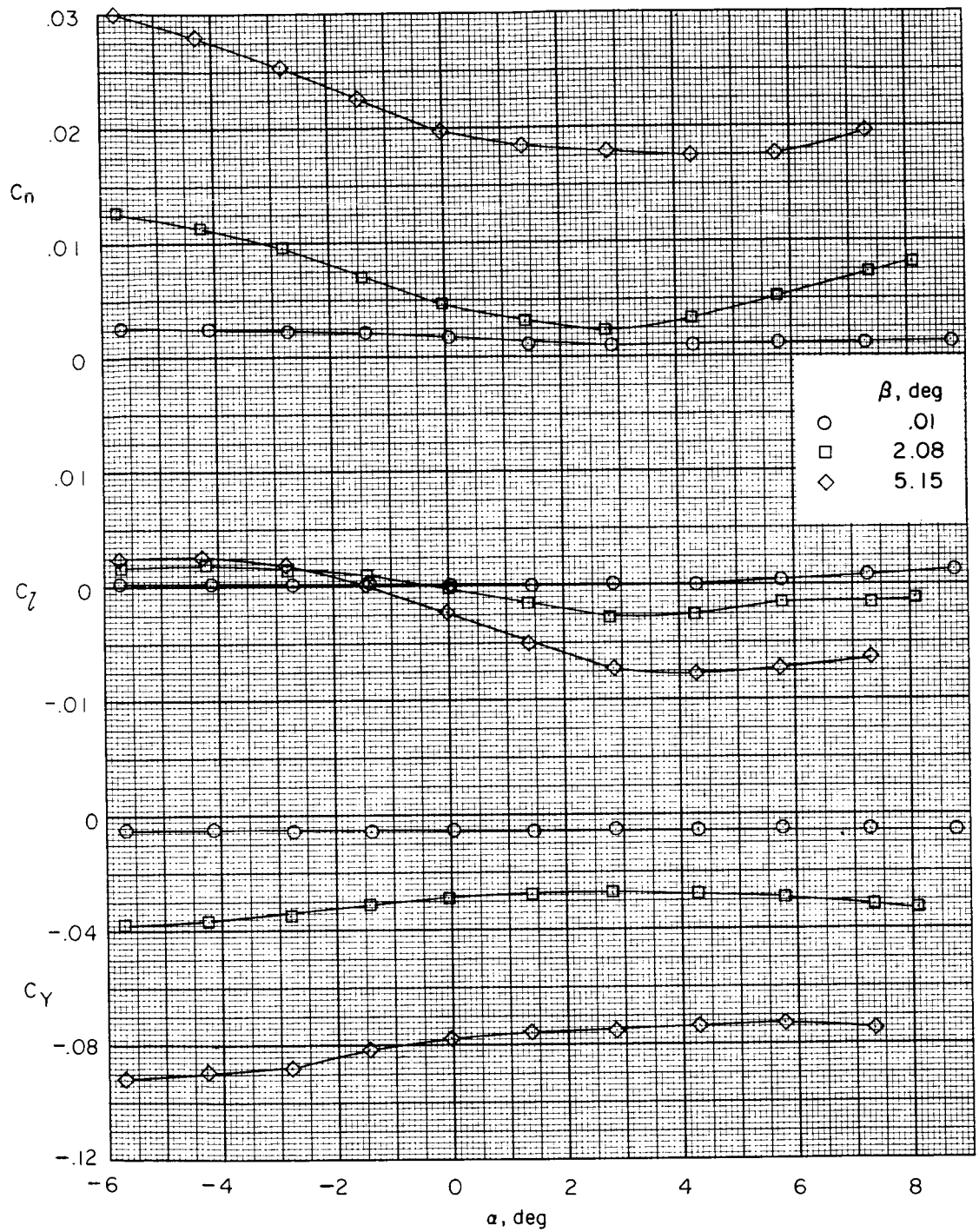
(d)  $M = 0.95$ .

Figure 5.- Continued.



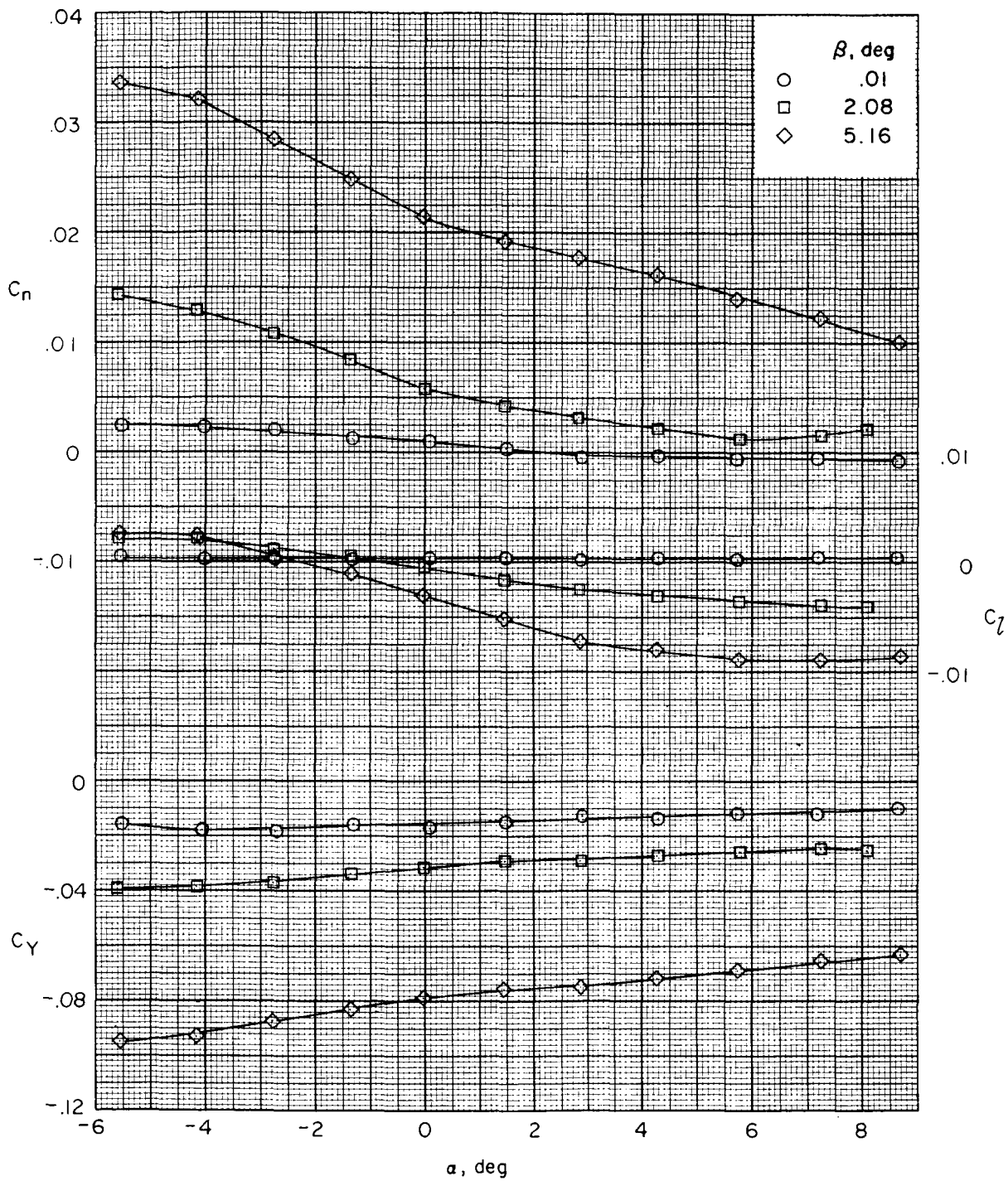
(e)  $M = 1.00$ .

Figure 5. - Continued.



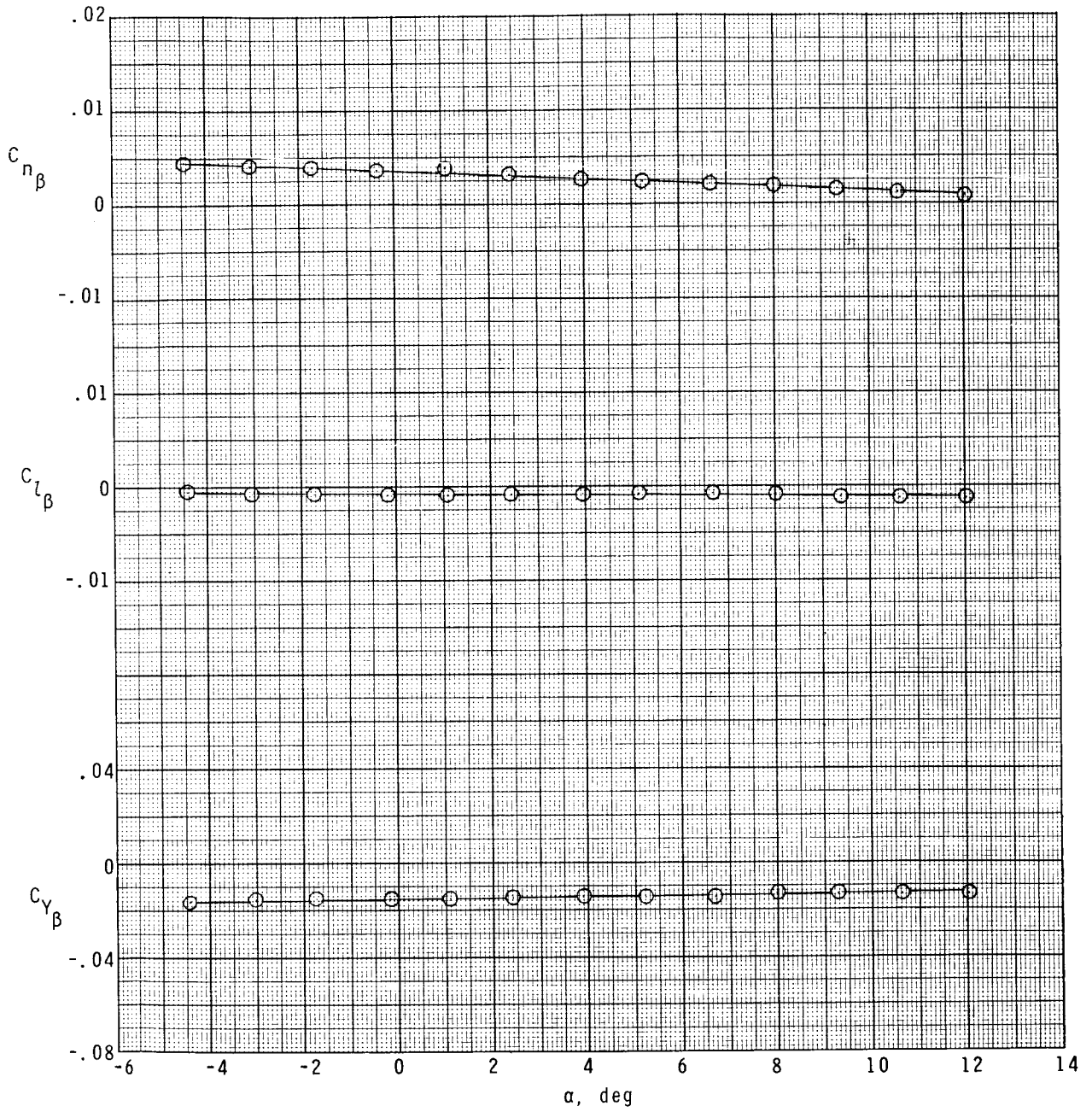
(f)  $M = 1.03$ .

Figure 5.- Continued.



(g)  $M = 1.20$ .

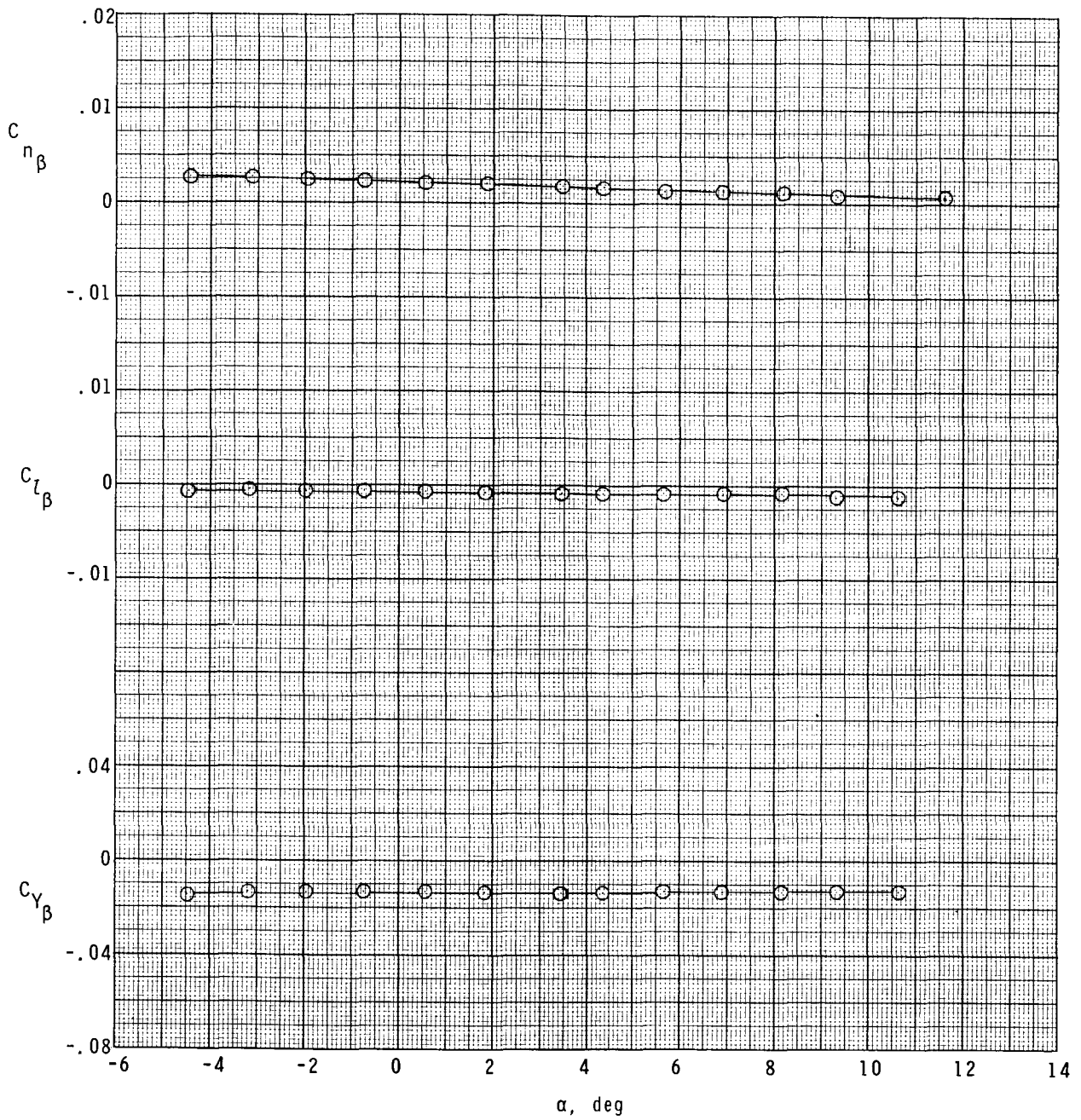
Figure 5.- Concluded.



(a)  $M = 2.00$ .

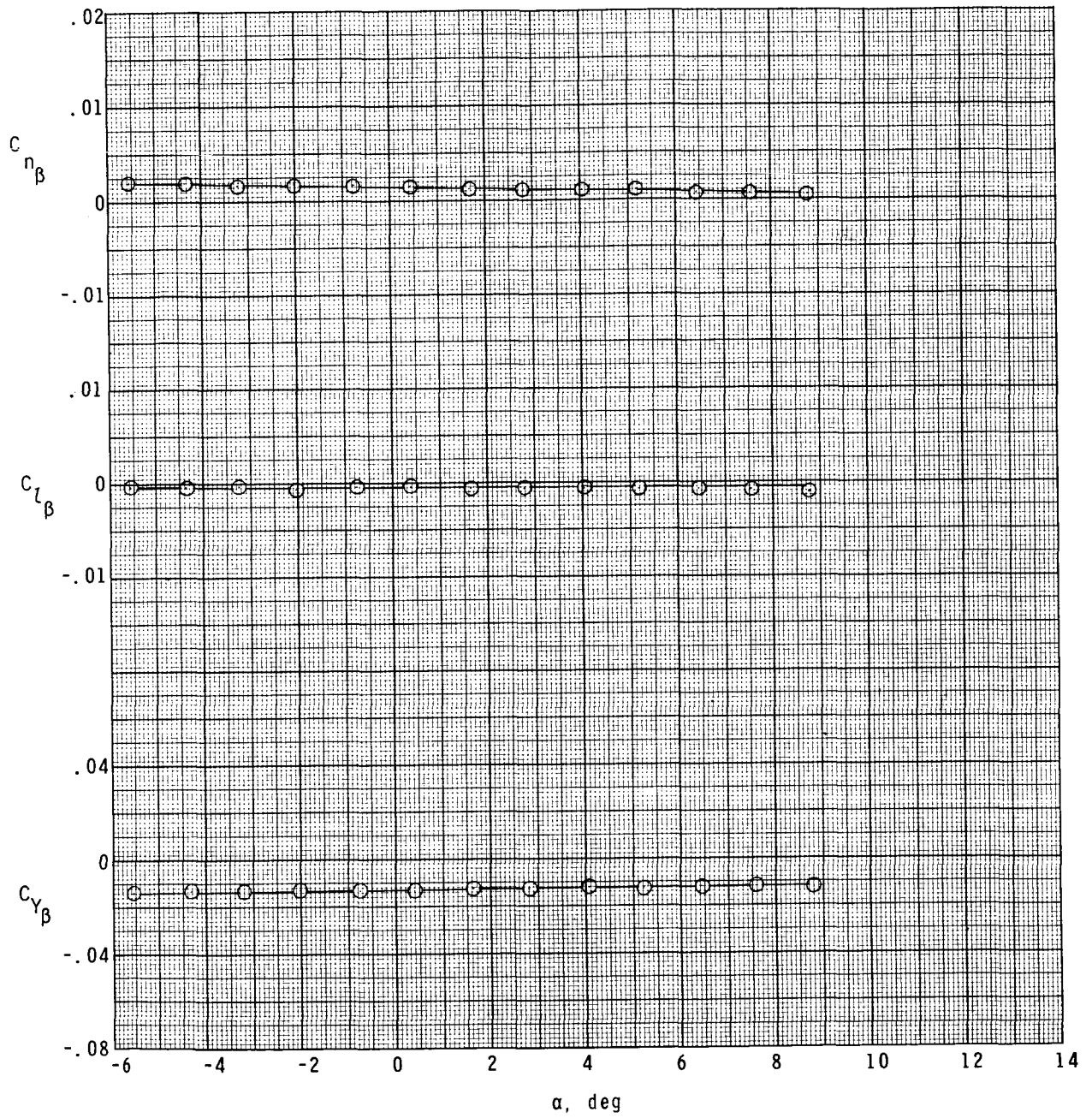
Figure 6.- Supersonic sideslip derivatives.





(b)  $M = 2.50$ .

Figure 6.- Continued.



(c)  $M = 2.86$ .

Figure 6.- Concluded.